MACROECONOMIC DRIVERS OF INFLATION EXPECTATIONS AND INFLATION RISK PREMIA

Jef Boeckx, Leonardo Iania, Joris Wauters

LIDAM Discussion Paper LFIN
2023 / 03

UCLouvain

LiDAM
LFIN | Louvain Institute of Data Analysis and Modeling in economics and statistics

LFIN

Voie du Roman Pays 34, L1.03.01 B-1348 Louvain-la-Neuve

Tel (32 10) 47 43 04

Email: lidam-library@uclouvain.be

https://uclouvain.be/en/research-institutes/lidam/lfin/publications.html

Macroeconomic drivers of Inflation Expectations and Inflation Risk Premia*

Jef Boeckx † Leonardo Iania ‡ Joris Wauters §

Preliminary and incomplete.

June 21, 2023

Abstract

We propose a new model to decompose inflation swaps into genuine inflation expectations and risk premiums. We develop a no-arbitrage term structure model with stochastic endpoints, separating macroeconomic variables into transitory parts and long-run, economically-grounded, determinants, such as the equilibrium real interest rate and the inflation target. Our estimations deliver new insights as to how macroeconomic variables affect market-based inflation expectation measures.

*We thank Alberto Plazzi and the participants to the seminars at the University of Calabria, Banca d'Italia and the European Central Bank for useful comments. The view expressed in this paper are solely those of the authors and not those of the National Bank of Belgium. All remaining errors are our responsibility. Leonardo Iania acknowledges the support of the following research grant: ARC 18/23-089.

†National Bank of Belgium
Email: Jef.Boeckx@nbb.be

‡UCLouvain, LFIN/CORE.
Email: leonardo.iania@uclouvain.be

§National Bank of Belgium
Email: Joris.Wauters@nbb.be

Contents

1 Introduction **3**

2 Modeling approach **5**
2.1 Term structure modeling 5
2.2 Dynamic system 7
2.3 Canonical representation 9

3 Empirical implementation **11**
3.1 Data and preliminary statistics 11
3.1.1 ILS data 11
3.1.2 Macroeconomic and survey data 13
3.2 Estimation strategy 15
3.2.1 State-space setting 15
3.2.2 Term structure model 18

4 Empirical Results **18**
4.1 Expected components and inflation risk premia 18
4.2 What drives ILS rates? 20
4.3 Campbell-Shiller tests 26

5 Conclusions **30**

A Appendix **31**

1 Introduction

Achieving price stability is at the core of major central banks' mandate. Historically, after the oil crises of the 70s, the world's leading central banks have contributed to a general decrease and subsequent stability in inflation rates, which averaged around 2% in rich OECD economies in the 2010s. However, inflation rates have surged since mid-2021 to multi-decade highs. In such an uncertain environment, gauging information about inflation expectations is key for central bankers, policymakers, and investors. For example, inflation-targeting central banks aim to monitor whether inflation expectations are anchored to the inflation target.

Unfortunately, measuring inflation expectations is not an easy task. Approximate measures can be derived indirectly from financial markets (market-based measures) and by surveying consumer and professional forecasters (survey-based measures). Both measures have pros and cons. Survey-based measures of expected inflation give an idea of the respondents' views about the inflation outlook, but they are not timely, as they are available at low frequencies, and, to a certain extent, not easy to interpret and to work with, as there is a great deal of heterogeneity among the different survey providers. The market-based measures of inflation expectations are extracted from financial contracts offering inflation hedges to market participants. They provide a timely and high-frequency measure of inflation expectations, and since market activities and actual trading determine them, they reflect the market's revealed - and not stated - concerns about future inflation. However, the inflation measures obtained from those contracts are inaccurate because they contain a risk premium, compensating investors for the uncertain returns in such contracts.

This paper proposes a model that decomposes the signal from financial measures of inflation expectations into genuine expectation components and changes in risk premia. The topic has attracted a considerable part of the macro-finance literature. Ang et al. (2008) develop a regime-switching Affine Term Structure Model (ATSM) with time-varying prices of risk and inflation to identify the relative contributions of real interest rates, expected inflation, and the inflation risk premium to changes in US nominal interest rates. Haubrich et al. (2012) estimate a model of nominal and real bond yield curves using data on Inflation-Linked Swap (ILS) rates, nominal Treasury yields, and inflation surveys. Christensen et al. (2010) and Joyce et al. (2010) build a standard affine model to jointly price nominal and real yields for the United States (US) and the United Kingdom (UK) and to study the evolution of the expected inflation and the inflation risk premium. Abrahams et al. (2016) extend the previous modeling framework to account for liquidity risk premia in inflation-linked government bonds. Carriero et al. (2018) introduce a shadow-rate term structure model for UK nominal and real yields to assess the impact of the recent Zero Lower-Bound (ZLB) period on inflation expectations and inflation risk premia. Hordahl and Tristani (2014) jointly model macroeconomic and term structure dynamics to estimate inflation risk premia and inflation expectations in the US and the Euro Area (EA). They consider data until 2014, hence excluding the recent low inflation period. More recently, Camba-Mendez and Werner (2017) developed model-free and model-based indicators for the inflation risk premium in the US and the EA using ILS data.

While this flourishing literature highlights the substantial effort devoted to disentangling inflation expectations from risk premia using market-based measures, some modeling and empirical questions are still open. For example: (i) What is the importance of long-term trend versus short-term macro dynamics in market-based measures of inflation expectations (and inflation risk premia)? (ii) What is the impact of international factors? (iii) Are the long-term and short-term determinants of EA and the US inflation risk premia and expectations similar? And finally, (iv) can we rely on the inflation risk premia extracted by these ATSM with or without macro variables?

To answer these questions, we build a novel ATSM with a stationary part of latent and macro variables and a random-walk block composed of long-run stochastic trends for trend inflation and the equilibrium real rate. As in the Joslin et al. (2011) setting, under the risk-neutral measure, ILS rates follow a low-dimensional factor structure with spanned factors, while the historical evolution of ILS rates, latent factors, macroeconomic variables, and stochastic trends is characterized by a higher-order vector correction model, with theory-grounded cointegration relationships. The model builds on the works of Dewachter and Iania (2011), who propose a Macro-Finance model of the US nominal yield curve including macroeconomic, liquidity-related, and return forecasting factors, and of Bauer and Rudebusch (2020), who extend the normalization setting of Joslin et al. (2011) to account for stochastic trends. Hence, our modeling framework allows us to express ILS rates and inflation risk premium as a function of (i) latent variables, namely the principal components of the ILS term structure; (ii) local macroeconomic variables, proxying for the target policy rate, inflation, and real activity; (iii) international trends on energy (oil) prices and commodity demand; and (iv) stochastic trends, linked to long term inflation expectations and the natural real rate. We estimate the model on monthly US and EA data, using a state-space setting whereby we exploit several mixed-frequency sources of information to identify the stochastic trends, such as the quarterly surveys data from the Surveys of Professional Forecasters and the monthly/bi-monthly and quarterly data from the Consensus Economics surveys. To ease the estimation burden and the over-fitting problem linked to parameter proliferation associated with the model's lag structure, we propose a penalized likelihood approach that shrinks high-order lags parameters (see Tibshirani, 1996; Fan and Li, 2001, among others, for early applications of this approach). Our model delivers several original results. First, the decomposition of ILS rates in expected component (EC) and inflation risk premium underscores that the latter is an important driver of ILS rates' variation, especially for the EA during the lowflation period. Furthermore, by further decomposing these two components in a deterministic and stochastic part (see Giannone et al., 2019), we point out that the EA latent factor models generate an oscillating behavior in the deterministic part of the EC. This problematic feature is absent in our model. Second, we use our framework to extract the expected and the inflation risk premium component of ILS rates -labeled EC and IRP, respectively - and to show how they relate to unspanned factors. The variance decompositions highlight that, for a 2-year maturity contract, the low-frequency movements of ILS rates are mainly driven by unspanned factors' innovations. However, its IRP component is dominated by spanned factors' shocks, which account for more than 50% of the high- and low-frequency movements. The historical decomposition highlights that unspanned factors are a primary source of ILS, EC, and IRPs' variation around key historical episodes such as the great financial crisis (GCF) and the 2010s oil price glut. Finally, we derive two types of Campbell and Shiller (1991) tests for the ILS market and show, depending on the market and type of tests, (i) mild evidence in favor of the expectations hypothesis and (ii) that a fully-fledged latent factor model without macro variables might not be adequate in correcting potential deviations from it. In contrast, the inflation risk premia extracted via our model often yield theoretically-consistent coefficients. In the rest of the paper, we outline our model, Section 2, present the dataset and the estimation strategy, Section 3, report and discuss our results, Section 4, and finally we draw the concluding remarks in Section 5.

2 Modeling approach

2.1 Term structure modeling

Defining the Inflation Linked Swap (ILS) contracts.
A zero-coupon ILS is a contract by which, at maturity, the floating leg counterpart receives a payment linked to the realized inflation rate over the duration of the contract (n), $\pi_{t+n,t} = \frac{P_{t+n}}{P_t} - 1$. In exchange, this party pays an amount linked to a fixed rate, $Y_{n,t}$, established at the initiation of the contract.[1] Since there is no exchange of money at the initiation of the contract, the expected value of the two payments should be equal:

$$\underbrace{\mathbb{E}_t^p\Big[M_{t,t+n}\big[(1+Y_{n,t})^n - 1\big]\Big]}_{\text{Fixed leg}} = \underbrace{\mathbb{E}_t^p\big[M_{t,t+n}\pi_{t+n,t}\big]}_{\text{Floating leg}} \quad p = \mathbb{P}, \mathbb{Q} \tag{1}$$

where $M_{t,t+n}$ is the stochastic discount factor. The equality reported in equation (1) is valid in probability settings adjusted for risk, risk-neutral probability measures $\mathbb{Q}$, or not, i.e. the historical probability measures $\mathbb{P}$. As shown by Camba-Mendez and Werner (2017), pricing the contract under the risk-neutral measure simplifies equation (1) as:

$$y_{n,t} = \frac{1}{n}\mathbb{E}_t^{\mathbb{Q}} e^{\sum_{j=1}^{n} \pi_{t+j}}, \tag{2}$$

where $y_{n,t}$ is the continuous time counterpart of $Y_{n,t}$ and π_{t+j} is the inflation rate between two consecutive periods, *t+j-1* and *t+j*. Equation (2) highlights that, in the risk-neutral probabilistic setting, the (continuously compounded) ILS rate is the expected average one-period inflation rate over the duration of the contract.

Accounting for risk.
We analyse the risk compensation in ILS contracts by focusing on the inflation risk premium and the forward risk premium, obtained via the decomposition of ILS and forward rates in expected and term premium components, respectively. We use our dynamic term structure modeling setting to decompose $y_{n,t}$ in EC and IRP components:

$$y_{n,t} = y_{n,t}^{EC} + y_{n,t}^{IRP} \tag{3}$$

Where $y_{n,t}^{EC}$ is the average expected inflation free of the inflation term premium, $y_{n,t}^{IRP}$, which represents the compensation required by market participants for their exposure to the model's risk factors. We obtain the decomposition in equation (3) in two steps. First, following Camba-Mendez and Werner (2017) we employ a Gaussian affine no-arbitrage

[1]The exchange of payments is performed at maturity, and the exact quantity of cash to exchange is proportional to the notional amount of the contract, which is multiplied by the realized inflation rate and the swap rate.

setting to price the ILS contracts. ILS rates are expressed as an affine function of the risk factors $\mathcal{Z}_t$, identified in Section 2.2, by setting (i) the one-period ILS rate, $y_{1,t}$, an affine function of $\mathcal{Z}_t$ and (ii) by assuming that the risk factors have affine Gaussian dynamics under both probability measures:

$$y_{1,t} = \rho_0 + \boldsymbol{\rho}_1' \mathcal{Z}_t \tag{4a}$$

$$\mathcal{Z}_t = \boldsymbol{\mu}^i + \boldsymbol{\Phi}^i \ \mathcal{Z}_{t-1} + \boldsymbol{\Sigma}\boldsymbol{\varepsilon}_t^i, \quad \boldsymbol{\varepsilon}_t^i \sim \mathcal{N}(\mathbf{0}, \boldsymbol{I}) \text{ and } i = \mathbb{Q}, \mathbb{P}, \tag{4b}$$

where ρ_0, $\boldsymbol{\rho}_1$, $\boldsymbol{\mu}^{\mathbb{P}}$, $\boldsymbol{\mu}^{\mathbb{Q}}$, $\boldsymbol{\Phi}^{\mathbb{P}}$, $\boldsymbol{\Phi}^{\mathbb{Q}}$ and $\boldsymbol{\Sigma}$ are (potential) model parameters while $\boldsymbol{I}$ is an identity matrix of conformable dimension. The parameters of equation (4b) under $\mathbb{Q}$ determine the pricing of the cross-sections of ILS rates, while the $\mathbb{P}$ parameters are key for the risk/term premium evolution. In our setting, the link between the two measures is obtained by assuming (i) essentially affine market prices of risk, $\boldsymbol{\Lambda}_t$, and (ii) a stochastic discount factor exponentially affine on the short-term ILS rate and $\boldsymbol{\Lambda}_t$:

$$\boldsymbol{\Lambda}_t = \boldsymbol{\Sigma}^{-1}\left(\boldsymbol{\lambda}_0 + \boldsymbol{\lambda}_{\mathbf{1}}\mathcal{Z}_t\right), \quad \boldsymbol{\mu}^{\mathbb{Q}} = \boldsymbol{\mu}^{\mathbb{P}} - \boldsymbol{\lambda}_0, \quad \boldsymbol{\Phi}^{\mathbb{Q}} = \boldsymbol{\Phi}^{\mathbb{P}} - \boldsymbol{\lambda}_{\mathbf{1}} \tag{5a}$$

$$M_{t,t+1} = \exp(-y_{1,t} - \frac{1}{2}\boldsymbol{\Lambda}_t'\boldsymbol{\Lambda}_t - \boldsymbol{\Lambda}_t'\boldsymbol{\Sigma}\boldsymbol{\varepsilon}_t^{\mathbb{P}}) \tag{5b}$$

Under these assumptions, it is possible to express $y_{n,t}$ as an affine function of the risk factors, $\mathcal{Z}_t$:

$$y_{n,t} = a_n + \boldsymbol{b}_n \mathcal{Z}_t \tag{6}$$

whereby the weights of (6) derive from the standard Riccati equations (see Ang and Piazzesi, 2003). Specifically, $a_n = -n^{-1}\mathrm{a}_n$ and $\boldsymbol{b}_n = -n^{-1}\mathrm{b}_n$

$$\mathrm{a}_n = \mathrm{a}_{n-1} + \mathrm{b}_{n-1}\boldsymbol{\mu}^{\mathbb{Q}} + \frac{1}{2}\mathrm{b}_{n-1}\boldsymbol{\Sigma}\boldsymbol{\Sigma}'\mathrm{b}_{n-1} - \rho_0 \tag{7a}$$

$$\mathrm{b}_n = \boldsymbol{\Phi}^{\mathbb{Q}'}\mathrm{b}_{n-1} - \boldsymbol{\rho}_1 \tag{7b}$$

Second, to obtain an expression for the EC of $y_{n,t}$, i.e. the part of the ILS rates net from the risk compensations, we first switch off risk compensation by setting to zero $\boldsymbol{\lambda}_0$ and $\boldsymbol{\lambda}_1$ in equation (5a). Subsequently, we derive a new set of loadings, a_n^{EC} and $\boldsymbol{b}_n^{EC}$, by iterating the Riccati equations with $\boldsymbol{\mu}^{\mathbb{P}}$ and $\boldsymbol{\Phi}^{\mathbb{P}}$ instead of $\boldsymbol{\mu}^{\mathbb{Q}}$ and $\boldsymbol{\Phi}^{\mathbb{Q}}$. As a result, the EC of $y_{n,t}$ is:

$$y_{n,t}^{EC} = a_n^{EC} + \boldsymbol{b}_n^{EC}\mathcal{Z}_t, \tag{8}$$

and the loadings for the term premium component of $y_{n,t}$ are obtained from equation (3) and equations (8) and (6):

$$y_{n,t}^{IRP} = y_{n,t} - y_{n,t}^{EC} \tag{9a}$$

$$= a_n - a_n^{EC} + (\boldsymbol{b}_n - \boldsymbol{b}_n^{EC})\mathcal{Z}_t \tag{9b}$$

$$= a_n^{IRP} + \boldsymbol{b}_n^{IRP}\mathcal{Z}_t. \tag{9c}$$

We define the forward risk premium as the risk premium on the n-k ILS rate k-periods from now. Labeling the latter forward rate as $y^f_{n-k,k,t}$, we can express it as:

$$\underbrace{y_{n-k,k,t}}_{\text{Forward rate}} = \frac{1}{n-k}(ny_{n,t} - ky_{k,t}) \tag{10a}$$

$$= \underbrace{\frac{1}{n-k}(n(y_{n,t} - y^{EC}_{n,t}) - k(y_{k,t} - y^{EC}_{k,t}))}_{\text{Forward risk premium}} + \underbrace{(\frac{1}{n-k}(ny^{EC}_{n,t} - ky^{EC}_{k,t}))}_{\text{Forward expected component}} \tag{10b}$$

$$= \underbrace{a^{FRP}_{n,k} + \boldsymbol{b}^{FRP}_{n,k}\mathcal{Z}_t}_{\text{Forward risk premium}} + \underbrace{a^{FEC}_{n,k} + \boldsymbol{b}^{FEC}_{n,k}\mathcal{Z}_t}_{\text{Forward expected component}} \tag{10c}$$

where (10a) follows from the accounting definition of forward rates, (10b) simply decomposes the ILS rates in expected and term premium components and, finally, the loadings in (10c) follow form (9c) and (8).

2.2 Dynamic system

Risk factors.
Our set of risk factors includes (up to) ten variables, divided in four categories: (i) two global variables $\mathbf{w}_t = [\Delta p^o_t, g^w_t]'$, proxying for changes in real oil prices and global real economic activity, respectively; (ii) three country-specific macro variables $\mathbf{m}_t = [\pi_t, g_t, i_t]'$, proxying for inflation, π_t, for economic activity, g_t, and for the policy rate, i_t; (iii) three ILS principal components,[2] the level, l_t, the slope, s_t, and the curvature, c_t, all stacked in $\mathbf{p}_t = [l_t, s_t, c_t]'$ and equal to $\mathbf{p}_t = W_p Y_t$, and (iv) two stochastic trends, one for inflation, π^*_t, and another for the equilibrium real rate, r^*_t, collected in the vector $\boldsymbol{\xi}_t = [\pi^*_t, r^*_t]'$ (see Dewachter and Iania, 2011). The time series evolution[3] of the global factors, the country-specific variables, and the principal components are summarized via a vector error-correction setting:

$$\begin{bmatrix} \mathbf{w}_t \\ \mathbf{m}_t \\ \mathbf{p}_t \end{bmatrix} = \underbrace{\sum_{v=1}^{\Upsilon} \begin{bmatrix} \boldsymbol{\Phi}^w_v & \boldsymbol{\Phi}^{wm}_v & \mathbf{0} \\ \boldsymbol{\Phi}^{mw}_v & \boldsymbol{\Phi}^m_v & \mathbf{0} \\ \boldsymbol{\Phi}^{pw}_v & \boldsymbol{\Phi}^{pm}_v & \boldsymbol{\Phi}^p_v \end{bmatrix} \begin{bmatrix} \mathbf{w}_{t-v} - \boldsymbol{\mu}^w - \boldsymbol{\Gamma}^w\boldsymbol{\xi}_t \\ \mathbf{m}_{t-v} - \boldsymbol{\mu}^m - \boldsymbol{\Gamma}^m\boldsymbol{\xi}_t \\ \mathbf{p}_{t-v} - \boldsymbol{\mu}^p - \boldsymbol{\Gamma}^p\boldsymbol{\xi}_t \end{bmatrix}}_{\text{Short-term component}} +$$

$$+ \underbrace{\begin{bmatrix} \boldsymbol{\mu}^w \\ \boldsymbol{\mu}^m \\ \boldsymbol{\mu}^p \end{bmatrix} + \begin{bmatrix} \boldsymbol{\Gamma}^w \\ \boldsymbol{\Gamma}^m \\ \boldsymbol{\Gamma}^p \end{bmatrix} \boldsymbol{\xi}_t}_{\text{Long-term component}} + \underbrace{\begin{bmatrix} \boldsymbol{\Sigma}^w & \mathbf{0} & \mathbf{0} \\ \boldsymbol{\Sigma}^{mw} & \boldsymbol{\Sigma}^m & \mathbf{0} \\ \boldsymbol{\Sigma}^{pw} & \boldsymbol{\Sigma}^{pk} & \boldsymbol{\Sigma}^p \end{bmatrix} \begin{bmatrix} \boldsymbol{\varepsilon}^w_t \\ \boldsymbol{\varepsilon}^m_t \\ \boldsymbol{\varepsilon}^p_t \end{bmatrix}}_{\text{Innovations}}, \qquad \begin{bmatrix} \boldsymbol{\varepsilon}^w_t \\ \boldsymbol{\varepsilon}^m_t \\ \boldsymbol{\varepsilon}^p_t \end{bmatrix} \sim \mathcal{N}(\mathbf{0}, \boldsymbol{I}), \tag{11}$$

where $\boldsymbol{I}$ is an identity matrix of conformable dimension. Equation (11) is the multivariate and multi-lag extension of Kozicki and Tinsley (2001) and Dewachter and Iania (2011).

[2] In Section 3.1.1 we report the loadings of the three principal components and show that they can be interpreted as level, slope and curvature.

[3] Note that the probability measure of reference is the historical one, but, to ease notation, we drop the superscript $\mathbb{P}$.

Short-term dynamics.
The short-term component of equation (11) describes how innovations to the system - brought about by the three sets of normally distributed shocks $\boldsymbol{\varepsilon}_t^w$, $\boldsymbol{\varepsilon}_t^m$, and $\boldsymbol{\varepsilon}_t^p$- propagate through time, causing a deviation of $\mathbf{w}_t$, $\mathbf{m}_t$, and $\mathbf{p}_t$ from their long-run values. Under suitable stability conditions, see infra, if no additional shocks hit the system these deviations converge to zero.

Three points are worth mentioning regarding the parameters included in the short-term and innovations components. First, $\boldsymbol{\Sigma}^w$,$\boldsymbol{\Sigma}^m$ and $\boldsymbol{\Sigma}^p$ are lower triangular, reflecting a Cholesky ordering of the shocks, with international factors being the most exogenous ones, followed by the country-specific factors and the principal components. For the international factors, the most exogenous innovation is the real oil price, while the ordering of country-specific factors follows the literature in assuming that supply shocks are the most exogenous, followed by demand shocks. Second, we impose that the ILS factors do not affect the evolution of the macro variables. This restriction is guaranteed by the Cholesky ordering and by imposing that $\boldsymbol{\Phi}_\upsilon^{wp}, \boldsymbol{\Phi}_\upsilon^{mp} = \mathbf{0}\ \forall \upsilon$. Third, following Joslin et al. (2013), we select a parsimonious one-lag structure on the ILS principal components by imposing that $\boldsymbol{\Phi}_\upsilon^{p} = \mathbf{0}\ \forall \upsilon > 1$.

Long-run dynamics.
To analyze the long-run behavior of $\mathbf{w}_t$, $\mathbf{m}_t$, and $\mathbf{p}_t$, we specify a random walk process for the stochastic trends and we conveniently write equation (11) in more compact form by defining $\mathbf{x}_t = [\mathbf{w}_t', \mathbf{m}_t', \mathbf{p'}_t]'$:

$$\mathbf{x}_t = \sum_{\upsilon=1}^{\Upsilon} \boldsymbol{\Phi}_\upsilon^x(\mathbf{x}_{t-\upsilon} - \boldsymbol{\mu}^x - \boldsymbol{\Gamma}^x \boldsymbol{\xi}_t) + \boldsymbol{\mu}^x + \boldsymbol{\Gamma}^x \boldsymbol{\xi}_t + \boldsymbol{\Sigma}^x \boldsymbol{\varepsilon}_t^x, \quad \boldsymbol{\varepsilon}_t^x \sim \mathcal{N}(\mathbf{0}, \boldsymbol{I}) \tag{12a}$$

$$\boldsymbol{\xi}_t = \boldsymbol{\xi}_{t-1} + \boldsymbol{\Sigma}^\xi \boldsymbol{\eta}_t, \quad \boldsymbol{\eta}_t \sim \mathcal{N}(\mathbf{0}, \boldsymbol{I}), \tag{12b}$$

where the subscripts x denote the compact vectors/matrices of equation (11). The long-run conditional expectation of $\mathbf{x}_{t+j}$, i.e. $\lim_{j\to\infty} \mathbb{E}^{\mathbb{P}}[\mathbf{x}_{t+j}|\mathcal{I}_t]$, relies on roots of the polynomial $\boldsymbol{\Phi}^x(\mathcal{L}) = \boldsymbol{\Phi}_1^x + \boldsymbol{\Phi}_2^x \mathcal{L} + ... + \boldsymbol{\Phi}_{\Upsilon-1}^x \mathcal{L}^{\Upsilon-1}$, defined in the lag operator $\mathcal{L}\mathbf{x}_t = \mathbf{x}_{t-1}$. If all roots of $I - \boldsymbol{\Phi}^x(\mathcal{L})$ lie outside the unit circle, then it follows that short-term component of equation (12a) (or equivalently equation (11)) shrinks to zero. As a consequence:

$$\lim_{j\to\infty} \mathbb{E}[\mathbf{x}_{t+j}|\mathcal{I}_t] = \boldsymbol{\mu}^x + \boldsymbol{\Gamma}^x \boldsymbol{\xi}_t, \tag{13}$$

which implies that the long-run expectations of the macro variables and the principal components incorporate a constant and a stochastic part, equal to $\boldsymbol{\Gamma}^x \boldsymbol{\xi}_t$ and governed by the cointegration matrices $\boldsymbol{\Gamma}^x = [\boldsymbol{\Gamma}^{w'}, \boldsymbol{\Gamma}^{m'}, \boldsymbol{\Gamma}^{p'}]'$, see equation (11), and the evolution of the stochastic trends $\boldsymbol{\xi}_t$, see equation (12b). Our three sets of assumptions for the long-run components of $\mathbf{x}_t$ are summarized below:

$$\boldsymbol{\mu}^{\mathbf{w}} = \begin{bmatrix} 0 \\ 0 \end{bmatrix}, \quad \boldsymbol{\mu}^{\mathbf{m}} = \begin{bmatrix} 0 \\ 0 \\ 0 \end{bmatrix}, \quad \boldsymbol{\mu}^{\mathbf{p}} = \begin{bmatrix} \mu^l \\ \mu^s \\ \mu^c \end{bmatrix}, \tag{14a}$$

$$\boldsymbol{\Gamma}^{\mathbf{w}} = \begin{bmatrix} 0 & 0 \\ 0 & 0 \end{bmatrix}, \quad \boldsymbol{\Gamma}^{\mathbf{m}} = \begin{bmatrix} 1 & 0 \\ 0 & 0 \\ 1 & 1 \end{bmatrix}, \quad \boldsymbol{\Gamma}^{\mathbf{p}} = \begin{bmatrix} \gamma^l & 0 \\ \gamma^s & 0 \\ \gamma^c & 0 \end{bmatrix} \tag{14b}$$

First, we assume stationarity for the demeaned global economic factors, $\mathbf{\Gamma}^{\mathbf{w}} = \mathbf{0}$ and $\boldsymbol{\mu}^{\mathbf{w}} = \mathbf{0}$. Second, for the local economic factors, we assume that the Fisher (1896) equation holds in the long run and we demeaned the measure of real activity, $\boldsymbol{\mu}^{\mathbf{m}} = \mathbf{0}$, implying:

$$\lim_{j\to\infty} \mathbb{E}[\pi_{t+j}|\mathcal{I}_t] = \pi_t^*, \tag{15a}$$

$$\lim_{j\to\infty} \mathbb{E}[g_{t+j}|\mathcal{I}_t] = 0, \tag{15b}$$

$$\lim_{j\to\infty} \mathbb{E}[i_{t+j}|\mathcal{I}_t] = \pi_t^* + r_t^*, \tag{15c}$$

Finally, to derive the long-term relationships for the ILS factors we start from the intuition that, under the historical probability measure, for any maturity, the long-run expected value of the ILS rates converges to

$$\lim_{j\to\infty} \mathbb{E}[y_{n,t+j}|\mathcal{I}_t] = \psi_n + \pi_t^*, \tag{16}$$

where ψ_n is a maturity-dependent constant accounting for potential premiums linked, for example, to liquidity. Next, since l_t, s_t, and c_t are a linear combination of the N ILS rates, collected in $Y_t = [y_{1,t}, ..., y_{N,t}]'$, we obtain:

$$\lim_{j\to\infty} \mathbb{E}[l_{t+j}|\mathcal{I}_t] = \mathrm{w}_l Y_t = \mathrm{w}_l(\boldsymbol{\psi} + \boldsymbol{\iota}\pi_t^*) = \mathrm{w}_l\boldsymbol{\psi} + \mathrm{w}_l\boldsymbol{\iota}\pi_t^*, \tag{17a}$$

$$\lim_{j\to\infty} \mathbb{E}[s_{t+j}|\mathcal{I}_t] = \mathrm{w}_l Y_t = \mathrm{w}_s(\boldsymbol{\psi} + \boldsymbol{\iota}\pi_t^*) = \mathrm{w}_s\boldsymbol{\psi} + \mathrm{w}_s\boldsymbol{\iota}\pi_t^*, \tag{17b}$$

$$\lim_{j\to\infty} \mathbb{E}[c_{t+j}|\mathcal{I}_t] = \mathrm{w}_c Y_t = \mathrm{w}_c(\boldsymbol{\psi} + \boldsymbol{\iota}\pi_t^*) = \mathrm{w}_c\boldsymbol{\psi} + \mathrm{w}_c\boldsymbol{\iota}\pi_t^*, \tag{17c}$$

where $\boldsymbol{\iota}$ is an N-dimensional column vector of ones and $\boldsymbol{\psi}$ is defined as $\boldsymbol{\psi} = [\psi_1, \psi_2, ...\psi_N]'$. The long-run relationships expressed in equations (17a) to (17c) have the following implication for $\boldsymbol{\mu}^{\mathbf{P}}$ and $\mathbf{\Gamma}^{\mathbf{P}}$. First, the elements of $\mathbf{\Gamma}^{\mathbf{P}}$ governing the cointegration relationship between the stochastic trend of inflation and the ILS principal components $(\gamma^l, \gamma^s, \gamma^c)$ are fixed to $\mathrm{w}_l\boldsymbol{\iota}$, $\mathrm{w}_s\boldsymbol{\iota}$, and $\mathrm{w}_c\boldsymbol{\iota}$, respectively. Second, the constant parts of the long-term components of $\mathbf{p}_t$, i.e. the elements of $\boldsymbol{\mu}^{\mathbf{P}}$, are simply a linear combination of the individual ψ's, which we treat as unknown parameters.

By defining $\mathbf{x}_t^{1:\Upsilon} = [\mathbf{x}_t', ..., \mathbf{x}_{t-\Upsilon+1}']'$ and $\mathcal{Z}_t = [\mathbf{x}_t^{1:\Upsilon'}, \boldsymbol{\xi}_t']'$ and by stacking the shocks in $\boldsymbol{\epsilon}_t^{\mathbb{P}} = [\boldsymbol{\varepsilon}_t^{x'}, \boldsymbol{\eta}_t']'$, we express the dynamic system in its companion form, which corresponds to equation (4b) under $\mathbb{P}$:

$$\mathcal{Z}_t = \boldsymbol{\mu}^{\mathbb{P}} + \boldsymbol{\Phi}^{\mathbb{P}}\mathcal{Z}_{t-1} + \boldsymbol{\Sigma}\boldsymbol{\epsilon}_t^{\mathbb{P}}, \quad \boldsymbol{\epsilon}_t^{\mathbb{P}} \sim \mathcal{N}(\mathbf{0}, \boldsymbol{I}). \tag{18}$$

The next section lays out the identification restrictions to equation (4b) under $\mathbb{Q}$.

2.3 Canonical representation

We adopt the normalization of Joslin et al. (2011), henceforth JSZ, and extend the setting of Bauer and Rudebusch (2020) to two stochastic trends, which we apply to the ILS market. The JSZ identification technique dramatically reduces the number of parameters of equation (4b) under $\mathbb{Q}$ via two sets of restrictions. First, it imposes the so-called spanning conditions, i.e. under $\mathbb{Q}$ only a few linear combinations of Y_t – $\mathbf{p}_t$ for our model – span the cross-section of ILS rates over time, i.e.:

$$\mathbb{E}^{\mathbb{Q}}[y_{n,t+j}|\mathcal{Z}_t] = \mathbb{E}^{\mathbb{Q}}[y_{n,t+j}|\mathbf{p}_t] \tag{19}$$

To satisfy condition (19) we impose that, in the risk-neutral dynamics, equations (4a) and (4b) depend only on $\mathbf{p}_t$:

$$y_{1,t} = \rho_0 + \boldsymbol{\rho}_1^{p'}\mathbf{p}_t, \tag{20a}$$

$$\mathbf{p}_t = \boldsymbol{\mu}^{\mathbb{Q},p} + \boldsymbol{\Phi}^{\mathbb{Q},p}\ \mathbf{p}_{t-1} + \boldsymbol{\Sigma}^p\boldsymbol{\varepsilon}_t^{\mathbb{Q},p}, \quad \boldsymbol{\varepsilon}_t^{\mathbb{Q},p} \sim \mathcal{N}(\mathbf{0}, \boldsymbol{I}_{N_p}), \tag{20b}$$

where the 3×1 vectors $\boldsymbol{\rho}_1^{p'}$ and $\boldsymbol{\mu}^{\mathbb{Q},p}$ and the 3×3 matrices $\boldsymbol{\Phi}^{\mathbb{Q},p}$ and $\boldsymbol{\Sigma}^p$ are the non-zero components of $\boldsymbol{\rho}_1'$, $\boldsymbol{\mu}^{\mathbb{Q}}$, $\boldsymbol{\Phi}^{\mathbb{Q}}$ and $\boldsymbol{\Sigma}$ in equation (4b) corresponding to $\mathbf{p}_t$. $\boldsymbol{\Sigma}$ also appears in equation (11) as the change of measure does not affect the variance of the shocks. Equations (20a) and (20b) imply that the ILS rates are an affine function of $\mathbf{p}_t$. Hence, equation (6) simplifies to:

$$y_{n,t} = a_n^p + \boldsymbol{b}_n^p\mathbf{p}_t, \tag{21}$$

where the loadings are obtained similarly as in equations (7a) and (7b), namely, $a_n^p = -n^{-1}\mathrm{a}_n^p$ and $\boldsymbol{b}_n^p = -n^{-1}b_n^p$ with:

$$\mathrm{a}_n^p = \mathrm{a}_{n-1}^p + b_{n-1}^p\boldsymbol{\mu}^{\mathbb{Q},p} + \frac{1}{2}b_{n-1}^p\boldsymbol{\Sigma^p}(b_{n-1}^p\boldsymbol{\Sigma^p})' - \rho_0 \tag{22a}$$

$$b_n^p = (\boldsymbol{\Phi}^{\mathbb{Q},p})'b_{n-1}^p - \boldsymbol{\rho}_1^p \tag{22b}$$

Looking at equations (20a), (20b), and (21), we notice that the spanning condition (19) is trivially satisfied as ILS rates at any maturity depend only on $\mathbf{p}_t$, which in turn, under $\mathbb{Q}$ depends only on its lagged value. The spanning assumption imposes a set of zero restrictions on the stochastic discount factor and the prices of risks, see equations (5a) and (5b), implying that:

$$M_{t,t+1} = \exp(-y_{1,t} - \frac{1}{2}\boldsymbol{\Lambda}_t^{p'}\boldsymbol{\Lambda}_t^p - \boldsymbol{\Lambda}_t^{p'}\boldsymbol{\Sigma}^p\boldsymbol{\varepsilon}_t^{\mathbb{P},p}) \tag{23a}$$

$$\boldsymbol{\Lambda}_t^p = \boldsymbol{\Sigma}^{p^{-1}}\left(\boldsymbol{\lambda}_0^p + \boldsymbol{\lambda}_1^p\mathcal{Z}_t\right). \tag{23b}$$

$$\boldsymbol{\lambda}_0^p = \boldsymbol{D}_p\boldsymbol{\mu}^{\mathbb{P}} - \boldsymbol{\mu}^{\mathbb{Q},p}, \tag{23c}$$

$$\boldsymbol{\lambda}_1^p = \boldsymbol{D}_p\boldsymbol{\Phi}^{\mathbb{P}} - [\mathcal{O}\ \boldsymbol{\Phi}^{\mathbb{Q},p}] \tag{23d}$$

with $\mathcal{O}$ a zero-entry matrix of conformable dimension and $\boldsymbol{D}_p = [\mathcal{O}\ \boldsymbol{I}_{3\times 3}]$ a matrix selecting the last three rows of $\boldsymbol{\mu}^{\mathbb{P}}$ and $\boldsymbol{\Phi}^{\mathbb{P}}$, i.e. the parts related to $\mathbf{p}_t$. In a nutshell, as the cross-section of ILS rates is summarized by $\mathbf{p}_t$, only shocks to those principal components are priced, see equation (23a). However, via equations (23a) and (23b), unspanned factors play a role in the pricing of those shocks, which are weighted by the 3×1 prices of risk vector $\boldsymbol{\Lambda}_t^p$, that in turn is linked to all the variables of the dynamic system (18) via the matrix $\boldsymbol{\lambda}_1^p$ of equation (23b).

To identify the risk-neutral parameters, we follow JSZ and impose a second set of restrictions identifying restrictions on the $\mathbb{Q}$-dynamics, so that the real-world dynamics can be estimated without restrictions. We start with $N = 3$ latent factors $\mathcal{X}_t$ and impose the following restrictions on their $\mathbb{Q}$-dynamics:

$$y_{1,t} = \iota \mathcal{X}_t, \quad \boldsymbol{\mu}^{\mathcal{X}} = \begin{bmatrix} \boldsymbol{\kappa}^{\mathcal{X}} \\ 0 \\ 0 \end{bmatrix}, \quad \boldsymbol{\Phi}^{\mathcal{X}} = \begin{bmatrix} \boldsymbol{\lambda}_1^{\mathcal{X}} & 0 & 0 \\ 0 & \boldsymbol{\lambda}_2^{\mathcal{X}} & 0 \\ 0 & 0 & \boldsymbol{\lambda}_3^{\mathcal{X}} \end{bmatrix}, \tag{24}$$

where ι is 1×3 vector of ones and the $\boldsymbol{\lambda}^{\mathcal{X}}$s are assumed to be less than one in absolute value. Subsequently, we obtain the term structure loadings related to $\mathcal{X}_t$, $A_{\mathcal{X}}$ and $B_{\mathcal{X}}$, and use the definition of $\mathbf{p}_t = W_p Y_t$ to obtain the loadings for $\mathbf{p}_t$ in function of the parameters in (24):

$$Y_t = (I - B_{\mathcal{X}}(W_p B_{\mathcal{X}})^{-1} W_p) A_{\mathcal{X}} + B_{\mathcal{X}}(W_p B_{\mathcal{X}})^{-1} \mathbf{p}_t \tag{25}$$

where $A_{\mathcal{X}}$ and $B_{\mathcal{X}}$ are the affine yield loadings on $\mathcal{X}_t$ and $W_p = [\mathrm{w}_l', \ \mathrm{w}_s', \ \mathrm{w}_c']'$.

3 Empirical implementation

3.1 Data and preliminary statistics

We estimate the model for the EA and the US using a mix of quarterly and monthly data from January 2005 to March 2022. Our empirical analysis combines four types of information: data on ILS rates, macroeconomic variables, survey forecasts, and model-based long-run trends.

3.1.1 ILS data

The swap series are from Bloomberg. We construct monthly series by taking the end-of-the-month data from the daily ILS rates with maturity 1 to 10, 12, 15, 20, 25, and 30 years, collected in the vector Y_t. Panel A (B) of Table 1 reports the summary statistics of the EA (US) 1-, 5-, 10-, and 30-year maturity ILS rates. In both regions, ILS rates are characterized by upward-sloping averages, decreasing volatility, short-term leptokurtosis (fat tails), and increasing persistence (EA 30-year rates are not more persistent than 10-year inflation swaps). US ILS rates are, on average, higher and less persistent than the EA counterparts. Short-term (long-term) US ILS rates[4] are 0.3% (0.5%) higher than the European ones, 1.7% vs. 1.4% (2.6% vs. 2.1%). Average US ILS rates are above the 2% target of the Federal Reserve. This difference might be due to the Federal Reserve's inflation target being based on the Personal Consumption Expenditure index, which delivers, on average, lower inflation rates than the Consumer Price Index, the underlying index in ILS contracts. Panels A and B of Figure 1 indicate that EA and US long-term ILS rates, i.e. above ten years of maturity, display a declining trend from the end of the first half of the '20s until September 2020. The recent COVID crisis and the Russian aggression against Ukraine reverted this trend, causing the longest observed inversion in the term structure of ILS rates in both regions.

[4] Short-term and long-term refer to 1-year and 30-year maturity, respectively.

Table 1: Summary statistics: ILS rates and PCs

	(A) EA ILS						(B) US ILS					
	μ	σ	s	k	ρ_1	ρ_3	μ	σ	s	k	ρ_1	ρ_3
1-year	0.014	0.009	0.961	7.902	0.924	0.728	0.017	0.012	-1.388	8.816	0.900	0.583
5-year	0.016	0.006	0.015	2.346	0.953	0.854	0.022	0.005	-0.661	4.661	0.919	0.665
10-year	0.018	0.005	-0.294	2.098	0.970	0.902	0.024	0.004	-0.581	2.832	0.927	0.746
30-year	0.021	0.004	-0.558	2.380	0.966	0.882	0.026	0.004	-0.272	2.173	0.942	0.826

	(C) EA PCs							(D) US PCs						
	μ	σ	s	k	ρ_1	ρ_3	$\frac{\lambda_j}{\sum \lambda_n}$	μ	σ	s	k	ρ_1	ρ_3	$\frac{\lambda_j}{\sum \lambda_n}$
PC 1	0.063	0.020	-0.038	2.702	0.955	0.843	0.907	0.075	0.021	-0.840	5.484	0.917	0.640	0.844
PC 2	-0.020	0.006	0.730	6.517	0.937	0.807	0.082	-0.045	0.008	-0.083	2.269	0.932	0.847	0.140
PC 3	0.010	0.002	-0.115	2.698	0.837	0.733	0.008	-0.002	0.002	-2.765	26.672	0.431	0.210	0.009

Notes: Panel A (B) reports the summary statistics of the EA (US) ILS rates with maturities of 1, 5, 10, and 30 years. Panel C (D) reports the summary statistics of the EA (US) first three principal components (PCs) of all the ILS rates. Symbols: μ = average; σ = standard deviation; s = skewness; k = kurtosis; ρ_1 = first order autocorrelation; ρ_3 = third order autocorrelation; λ_j = eigenvalue associated with the j-*th* principal component.

From vector Y_t, we extract for each country the first three principal components $PC1_t$, $PC2_t$, and $PC3_t$, whose statistics, plots and loadings are reported in panels C and D of Table 1, in panels C and D, and in panels E and F of Figure 1, respectively. Notably, in both regions, the first three principal components capture more than 99% of the total variation, with the first factor responsible for approximately 90% of the variation in the EA and 84% for the US data.

Figure 1: ILS rates, principal components, and loadings.

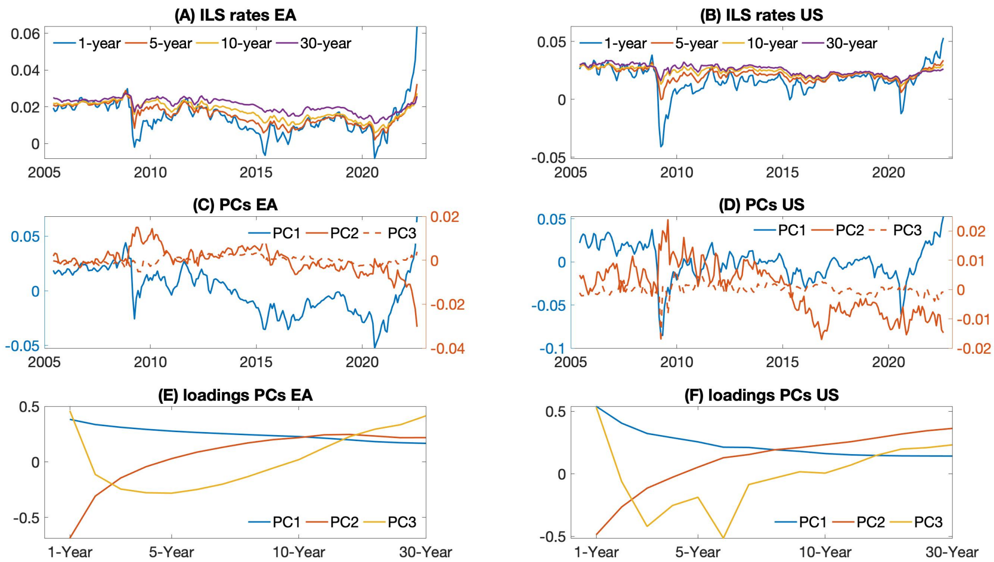

Notes: Panel A (B) plots the EA (US) ILS rates with maturities of 1, 5, 10, and 30 years. Panel C (D) depicts the first three principal components of all the EA (US) ILS rates while Panel E (F) reports their respective loadings.

For both ILS term structures, the loadings of the first factor are the (exponentially decaying) weighted averages of all ILS rates, while the second factors load negatively on short-term maturities and positively on long-term ones, giving them the interpretation of level and slope factors. The third factor is the difference between (i) the average of long- and short-term ILS rates and (ii) medium-term ones, i.e. the common shape of yield curves curvature factors. By summing up the weights for each factor/country, i.e. w_l, w_s and w_c, the resulting entries for the cointegration matrices $\mathbf{\Gamma^P}$s of equation (14b) are:

$$\mathbf{\Gamma}^{\mathbf{P},EA} = \begin{bmatrix} 3.8 & 0 \\ 0.8 & 0 \\ 0.3 & 0 \end{bmatrix} \qquad \mathbf{\Gamma}^{\mathbf{P},US} = \begin{bmatrix} 3.5 & 0 \\ 1.6 & 0 \\ -0.1 & 0 \end{bmatrix}.$$

3.1.2 Macroeconomic and survey data

Macroeconomic data.

Macroeconomic variables are divided into country-specific and international factors. Country-specific factors are obtained from the Federal Reserve Economic Data (FRED) database maintained by the Federal Reserve Bank of St. Louis for the US and from the ECB Statistical Data Warehouse (SDW) for the EA. We proxy the inflation factor via the month-on-month growth rate of the inflation index underlying the ILS contracts, i.e. the seasonally-adjusted Harmonised Index of Consumer Prices (HICP) for the EA and the Consumer Price Index (CPI) for the US[5], while the real activity measure is given by the month-on-month growth rate of the Industrial Production Index.[6] As risk-free rates, we use the one-year t-bill rate[7] International factors are (i) the monthly growth rate of the nominal price of oil (spot) for West Texas Intermediate (WTI), retrieved from the FRED[8] and deflated by the U.S. CPI[9] and (ii) the Baumeister et al. (2022)'s measure of global real economic conditions.

[5]FRED mnemonic: CPILFESL; SDW mnemonic: ICP.M.U2.Y.000000.3.INX.

[6]FRED mnemonic: INDPRO; SDW mnemonic: STS.M.I8.Y.PROD.NS0020.4.000.

[7]FRED mnemonic: DTB1YR. Since the series is discontinued till June 2008, prior to that date we use the one-year rate obtained from Liu and Wu (2021).

[8]FRED mnemonic: OILPRICE.

[9]FRED mnemonic: CPIAUCSL (consumer price index for all urban consumers: all items, index 1982-1984 = 100).

Figure 2: Observable variables

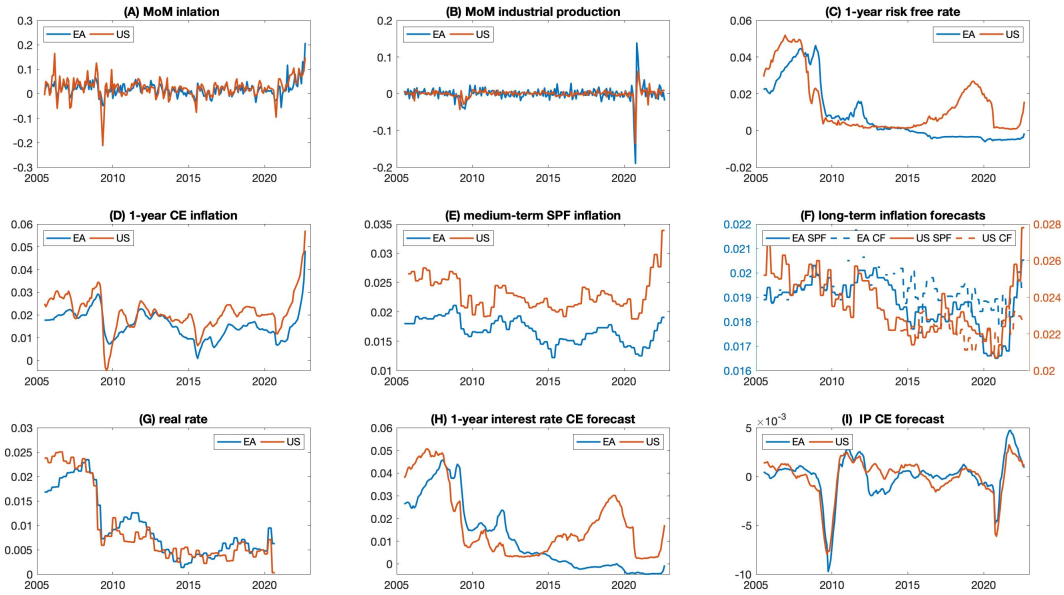

Notes: The top panels report the observed series of month-on-month inflation, industrial production growth (panels A and B, respectively), and the one-year risk-free rate (panel C). The middle panels depict the inflation surveys. Panel D plots the monthly Consensus Economics (CE) one-year-ahead inflation forecast, panel E reports the two (five) year inflation Survey of Professional Forecast (SPF) for the EA (US), and panel F depicts (i) the five (ten) year inflation forecast from the SPF for the EA (US), and (ii) the long-term (above five years) CE inflation forecasts. Finally, the bottom panels show the quarterly Holston et al. (2017) natural rate of interest (panel G), and the monthly CE one-year risk-free rate (panel H) and industrial production (panel I) forecast. In each panel, blue lines refer to EA data, while red lines are for US data.

Surveys and model-based series.
Finally, we exploit the information contained in surveys, and we employ the quarterly natural interest rate constructed by Holston et al. (2017) with the goal to (i) identify the two stochastic trends and (ii) identify the value of real activity at the beginning of the Covid-19 period.

To fix notations, the surveys forecasts for a variable x are labelled as: $\mathbb{E}_t^{\mathcal{S}} x_{t+t_1 \to t+t_2}$, where (i) $\mathcal{S}$ indicates the source from where the subjective forecasts are obtained, and (ii) $t+t_1$ and $t+t_2$ are the beginning and the end of the forecasting period, respectively, expressed in months. For each country, we use two survey providers: the Survey of Professional Forecasters (SPF) and the Consensus Economics (CE) forecasts, i.e. $\mathcal{S} = \{SPF, CE\}$. EA SPF is from The European Central Bank (ECB) provides the EA SPF, while Philadelphia Federal Reserve is the provider of the US SPF. From the ECB (Philadelphia FED) SPFs, we select the year-on-year inflation forecast in two and five years (average inflation over the next five and ten years), which we label $\mathbb{E}_t^{\text{SPF}} \pi_{t+t_1 \to t+t_2}$, with $t_1 = \{12, 48\}$ and $t_2 = \{24, 60\}$ ($t_1 = \{1, 1\}$ and $t_2 = \{60, 120\}$) months.We use two sets of CE surveys, the short-term and long-term forecasts. Short-term CE forecasts for the next-year inflation rate, $\mathbb{E}_t^{\text{CE}} \pi_{t+1 \to t+12}$, industrial production, $\mathbb{E}_t^{\text{CE}} g_{t+1 \to t+12}$, and one-year interest rates, $\mathbb{E}_t^{\text{CE}} i_{t+1 \to t+12}$, are proxied by an extrapolation from (i) the current and next calendar year forecasts and (ii) from the next-year forecast for the 3-month and

10-year interest rates, respectively:

$$\mathbb{E}_t^{\text{CE}}\pi_{t+1\to t+12} = \frac{(13-\mathsf{m}(t))-1}{12}\mathbb{E}_t^{\text{CE}}\pi_{\mathsf{y}(t)} + \frac{(\mathsf{m}(t)-1)}{12}\mathbb{E}_t^{\text{CE}}\pi_{\mathsf{y}(t)+1} \tag{26a}$$

$$\mathbb{E}_t^{\text{CE}}g_{t+1\to t+12} = \frac{(13-\mathsf{m}(t)-1)}{12}\mathbb{E}_t^{\text{CE}}g_{\mathsf{y}(t)} + \frac{(\mathsf{m}(t)-1)}{12}\mathbb{E}_t^{\text{CE}}g_{\mathsf{y}(t)+1} \tag{26b}$$

$$\mathbb{E}_t^{\text{CE}}i_{t+12} = \mathbb{E}^{\text{CE}}i_{t+12}^3 + \frac{\mathbb{E}_t^{\text{CE}}i_{t+12}^{120} - \mathbb{E}_t^{\text{CE}}i_{t+12}^3}{120-3}(12-3) \tag{26c}$$

In equations (26a) and (26b) $\mathsf{y}(t)$ and $\mathsf{m}(t)$ are the calendar years and months related to time t, respectively. The expression approximates fixed-horizon forecasts as a weighted average of fixed-event forecasts (see Dovern et al., 2012). Equation (26c) approximates the forecast of the 1-year interest rate, $\mathbb{E}_t^{\text{CE}}i_{t+12}$, as the weighted average of the forecast of the 3-month and 10-year interest rates in one year, $\mathbb{E}_t^{\text{CE}}i_{t+12}^3$ and $\mathbb{E}_t^{\text{CE}}i_{t+12}^{120}$, respectively. The implicit assumption is that the forecasters-implied yield curve has the same slope for all maturities. Long-term CE forecasts are short-term interest rates and inflation expectations in five to ten years, $\mathbb{E}_t^{\text{CE}}i_{t+60\to t+120}^3$ and $\mathbb{E}_t^{\text{CE}}\pi_{t+60\to t+120}$. Finally, our last observed variable is the quarterly natural interest rate constructed by Holston et al. (2017), $\tilde{r}_t^*$, which helps identify the stochastic trend for the interest rate.

3.2 Estimation strategy

The estimation of our term structure model involves two steps: (i) the identification of the stochastic trends and the fitting of risk factors' dynamic system (18) and (ii) the pricing of the ILS contracts via the multivariate version of equation (21). The first step is performed in a state-space setting, while the second one maximizes the fit of ILS rates via (a constrained) linear system.

3.2.1 State-space setting

Measurement Equation.
We estimate the system outlined in Section 2.2 via state-space setting, whereby the state variables, $\mathcal{Z}_t$, see (18), are linearly related to a set of observable variables, $\mathcal{Y}_t$:

$$\mathcal{Y}_t = \mathbf{a} + \mathbf{B}\mathcal{Z}_t + \mathbf{\Sigma}^{\mathcal{Y}}\boldsymbol{\epsilon}_t^{\mathcal{Y}}, \quad \boldsymbol{\epsilon}_t^{\mathcal{Y}} \sim \mathcal{N}(\mathbf{0}, \boldsymbol{I}), \tag{27}$$

where $\mathbf{\Sigma}^{\mathcal{Y}}$ is a diagonal matrix of standard deviations. The observed series and their corresponding loadings, $\mathbf{a}$ and $\mathbf{B}$, are divided in four blocks:

$$\mathcal{Y}_t' = \begin{bmatrix}\mathcal{Y}_t^{\mathcal{O}'} & \mathcal{Y}_t^{\pi'} & \mathcal{Y}_t^{g'} & \mathcal{Y}_t^{i'}\end{bmatrix} \tag{28a}$$

$$\mathbf{a}' = \begin{bmatrix}\mathbf{a}^{\mathcal{O}'} & \mathbf{a}^{\pi'} & \mathbf{a}^{g'} & \mathbf{a}^{i'}\end{bmatrix} \tag{28b}$$

$$\mathbf{B}' = \begin{bmatrix}\mathbf{B}^{\mathcal{O}'} & \mathbf{B}^{\pi'} & \mathbf{B}^{g'} & \mathbf{B}^{i'}\end{bmatrix}. \tag{28c}$$

The first block, $\mathcal{Y}_t^{\mathcal{O}}$, includes the observed data, i.e. $\mathbf{w}_t$, $\mathbf{m}_t$, and $\mathbf{p}_t$:

$$\mathcal{Y}_t^{\mathcal{O}} = \begin{bmatrix}\Delta p_t^o & g_t^w & \pi_t & g_t & i_t & l_t & s_t & c_t\end{bmatrix}', \tag{29a}$$

$$\mathbf{a}^{\mathcal{O}} = \begin{bmatrix}0 & 0 & 0 & 0 & 0 & 0 & 0 & 0\end{bmatrix}', \tag{29b}$$

$$\mathbf{B}^{\mathcal{O}} = \begin{bmatrix}\iota^{\Delta p^{o'}} & \iota^{g^{w'}} & \iota^{\pi'} & \iota^{g'} & \iota^{i'} & \iota^{l'} & \iota^{s'} & \iota^{s'}\end{bmatrix}'. \tag{29c}$$

Since the stationary state variables are observed without error, the elements of $\mathbf{a}^{\mathcal{O}}$ are set to zero while $\mathbf{B}^{\mathcal{O}}$ is made of row vectors selecting the respective observed variables from the state vector, $\mathcal{Z}_t$. For example, for the macro series, these restrictions correspond to:

$$\iota^{\pi} = \begin{bmatrix} 0 & 0 & 1 & 0 & 0 & 0 & \dots & 0 \end{bmatrix} \tag{30a}$$
$$\iota^{g} = \begin{bmatrix} 0 & 0 & 0 & 1 & 0 & 0 & \dots & 0 \end{bmatrix} \tag{30b}$$
$$\iota^{i} = \begin{bmatrix} 0 & 0 & 0 & 0 & 1 & 0 & \dots & 0 \end{bmatrix}. \tag{30c}$$

To account for the large deviation of the industrial production series at the beginning of the Covid-19 period, we impose that g_t is not observed from March 2020 to August 2020. The third block, see infra, identifies g_t over that period. The second block includes the four inflation survey data from the SPF and from the CF:

$$\mathcal{Y}_t^{\pi} = \begin{bmatrix} \mathbb{E}_t^{\text{SPF}} \pi_{t+t_1 \to t+t_2} & \mathbb{E}_t^{\text{SPF}} \pi_{t+t_3 \to t+t_4} & \mathbb{E}_t^{\text{CE}} \pi_{t+1 \to t+12} & \mathbb{E}_t^{\text{CE}} \pi_{t+61 \to t+120} \end{bmatrix}', \tag{31a}$$
$$\mathbf{a}^{\pi} = \begin{bmatrix} \iota^{\pi} \bar{\mathbf{a}}_{t_1 \to t_2} & \iota^{\pi} \bar{\mathbf{a}}_{t_3 \to t_4} & \iota^{\pi} \bar{\mathbf{a}}_{1 \to 12} & \iota^{\pi} \bar{\mathbf{a}}_{61 \to 120} \end{bmatrix}', \tag{31b}$$
$$\mathbf{B}^{\pi} = \begin{bmatrix} \iota^{\pi} \bar{\mathbf{B}}'_{t_1 \to t_2} & \iota^{\pi} \bar{\mathbf{B}}'_{t_3 \to t_4} & \iota^{\pi} \bar{\mathbf{B}}'_{1 \to 12} & \iota^{\pi} \bar{\mathbf{B}}'_{61 \to 120} \end{bmatrix}'. \tag{31c}$$

where (i) for the EA (US) t_1, t_2, t_3, and t_4 are equal to 12, 24, 48 and 60 months (1, 60, 1, and 120 months), respectively, and ι^{π}, defined in (30a) selects the inflation components of $\bar{\mathbf{a}}'_{\tau_1 \to \tau_2}$ and $\bar{\mathbf{B}}'_{\tau_1 \to \tau_2}$. For a generic forecasting horizon ranging form τ_1 to τ_2, the loadings $\bar{\mathbf{a}}'_{\tau_1 \to \tau_2}$ and $\bar{\mathbf{B}}'_{\tau_1 \to \tau_2}$ are the model-implied average forecasts of the state variables over the period $[\tau_1, \tau_2]$:

$$\bar{\mathbf{a}}_{\tau_1 \to \tau_2} = \frac{1}{\tau_2 - \tau_1 + 1} \sum_{H=\tau_1}^{\tau_2} \left[\sum_{h=1}^{H} \mathbf{\Phi}^{h-1} \right] \boldsymbol{\mu}, \tag{32a}$$
$$\bar{\mathbf{B}}_{\tau_1 \to \tau_2} = \frac{1}{\tau_2 - \tau_1 + 1} \sum_{H=\tau_1}^{\tau_2} \mathbf{\Phi}^{H} \tag{32b}$$

As we observed that the 12-month CE forecasts were substantially more volatile than the SPF's, we (i) scale its model-implied counterpart by a factor β^{CE} and (ii) we add to it a level factor, α^{CE}, to account for shifts in the level of the model-implied forecast brought about by the scaling factor β^{CE}.

The third block includes information related to industrial production around the first period of the Covid-19 crisis, namely the period from March 2020 to August 2020. During this period, we treat the series of Industrial Production Indexes as a latent factor which is noisily observed via (i) the realized month-on-month growth rate of the Industrial Production Index from March 2020 to August 2021 and (ii) its year-on-year CE forecast, $\mathbb{E}_t^{\text{CE}} g_{t+12}$. The resulting measured variables and loadings are:

$$\mathcal{Y}_t^{g} = \begin{bmatrix} \tilde{g}_t & \mathbb{E}_t^{\text{CE}} \tilde{g}_{t+1 \to t+12} \end{bmatrix}', \tag{33a}$$
$$\mathbf{a}^{g} = \begin{bmatrix} \alpha^{\tilde{g}} & \iota^{g} \bar{\mathbf{a}}_{1 \to 12} \end{bmatrix}', \tag{33b}$$
$$\mathbf{B}^{g} = \begin{bmatrix} \beta^{\tilde{g}} \iota^{g} & \iota^{g} \bar{\mathbf{B}}'_{1 \to 12} \end{bmatrix}', \tag{33c}$$

where the parameters $\alpha^{\tilde{g}}$ and $\beta^{\tilde{g}}$ allow the observed industrial production growth to differ from the latent one, the loadings $\bar{\mathbf{a}}_{1\to12}$ and $\bar{\mathbf{B}}_{1\to12}$ are from equations (32a) and (32b), and ι^{g} is defined in equation (30b).

The last block, $\mathcal{Y}^{i}_{t}$, includes three types of information, coming from two sources: (i) the short- and long-term CE interest rates forecasts, and (ii) the Holston et al. (2017) measure of the equilibrium real rate. The resulting block of the measurement equations includes:

$$\mathcal{Y}^{i}_{t} = \begin{bmatrix} \mathbb{E}^{\text{CE}}_{t} i^{12}_{t+12} & \mathbb{E}^{\text{CE}}_{t} i^{12}_{t+61\to t+120} & \tilde{r}^{*}_{t} \end{bmatrix}', \tag{34a}$$

$$\mathbf{a}^{i} = \begin{bmatrix} \iota^{i}\bar{\mathbf{a}}_{12} & \iota^{i}\bar{\mathbf{a}}_{61\to120} & \alpha^{\tilde{r}} \end{bmatrix}', \tag{34b}$$

$$\mathbf{B}^{i} = \begin{bmatrix} \iota^{i}\bar{\mathbf{B}}'_{12} & \iota^{i}\bar{\mathbf{B}}'_{61\to120} & \beta^{\tilde{r}} \end{bmatrix}', \tag{34c}$$

where the loading of the interest forecasts are obtained via the equations (32a) and (32b), while $\alpha^{\tilde{r}}$ and $\beta^{\tilde{r}}$ account for potential differences in mean and volatility between our model-implied stochastic trend for the real rate and the Holston et al. (2017)'s measure. Finally, given the identifying assumption related to the measurement equation, the matrix of the standard deviation of the measurement errors is defined as:

$$\mathbf{\Sigma}^{\mathcal{Y}} = \text{diag}\begin{bmatrix} 0 & \sigma^{g} & \sigma^{\text{SPF}^{\pi}_{1}} & \dots & \sigma^{\tilde{r}} \end{bmatrix},$$

with all non-zero elements except for the equations of the observed inflation and short-term interest rate.

Likelihood function.

We estimate the model composed by equations (27) and (18) using a penalized likelihood approach, a method that is widely used in high-dimensional statistical modeling (see Tibshirani, 1996; Fan and Li, 2001, among others). The penalized log-likelihood is composed of two parts:

$$l \propto \underbrace{-\frac{1}{2}\sum_{t=\Upsilon}^{T}(\ln|\boldsymbol{F}_{t}| + \boldsymbol{v}'_{t}\boldsymbol{F}^{-1}_{t}\boldsymbol{v}_{t})}_{\text{KF-EPD}} + \underbrace{p(\mathbf{\Phi}) + p(\mathbf{\Sigma}^{\xi}) + p(\mathbf{\Sigma}^{\mathcal{Y}}) + \sum(p(\alpha) + p(\beta))}_{\text{Penalty}}. \tag{35}$$

The component labeled KF-EPD is obtained by exploiting the Gaussian nature of the linear state-space model. It represents the sum of the likelihood of the Kalman Filter's prediction errors, $\boldsymbol{v}_{t}$, whose variance is given by $\boldsymbol{F}_{t}$. The functional forms of $\boldsymbol{v}_{t}$ and $\boldsymbol{F}_{t}$ derive from the Kalman Filter's recursions (Harvey, 1990, page 125).

The second part of the log-likelihood includes the penalties for the system's (block of) parameters. The first set of penalties relates to the elements of $\mathbf{\Phi}$. For these parameters, we adopt a $\|\text{L}\|^{2}$ regularization, whereby the (scaled) elements of $\mathbf{\Phi}$ are shrunk to zero via the following quadratic penalty function:

$$p(\mathbf{\Phi}) = \sum_{\upsilon=1}^{\Upsilon}\sum_{j=1}^{3}\sum_{i=1}^{3}\lambda_{\upsilon}(i,j)\left[\upsilon\frac{\tilde{\phi}_{\upsilon}(i,j)}{\varphi_{i,j}}\right]^{2}, \quad \lambda_{\upsilon}(i,j) = \begin{cases} \zeta^{2}_{1} & \forall i = j \\ \zeta^{2}_{1}\zeta^{2}_{2} & \text{otherwise.} \end{cases} \tag{36}$$

In equation (36), the interpretations and values of the scaling coefficients $\varphi_{i,j}$, ζ_{1} and ζ_{2} are as follows. The coefficients $\varphi_{i,j}$ account for the fact that the macro series are not standardized and hence might have different sample variances. We set their values to the outer product of the standard deviations of $\hat{\mathbf{m}}_t$, the deviation of the macro variables from the stochastic trends extrapolated from the surveys series. To penalize model complexity, we divided $\varphi_{i,j}$ by the lag of the coefficients it refers to, implying stronger regularization for additional lags added to the model. The coefficients ζ_1 and ζ_2 control the overall shrinkage and the penalization for the interaction coefficients, respectively. Following the Bayesian literature, we set their values to $\zeta_1 = \zeta_2 = \sqrt{2}$.

The additional penalties relate to the identification of the stochastic trends and are linked to (i) the standard deviations of the stochastic trends, $\mathbf{\Sigma}^{\xi}$, and of the measurement equation (27), $\mathbf{\Sigma}^{y}$, and (ii) to the additional coefficients of the measurement equations, namely α^{CE}, β^{CE}, $\alpha^{\tilde{g}}$, $\beta^{\tilde{g}}$, $\alpha^{\tilde{g}}$, $\beta^{\tilde{g}}$, $\alpha^{\tilde{r}}$ and $\beta^{\tilde{r}}$. For the standard deviations we use the following penalty function:

$$p(\boldsymbol{\sigma}^k) = \lambda^k \left[\ln \boldsymbol{\sigma}^k - \ln \bar{\boldsymbol{\sigma}}^k\right]^2, \quad \{\lambda^k, \ln \bar{\boldsymbol{\sigma}}^k\} = \begin{cases} \{100, \ln \hat{\boldsymbol{\sigma}}^k\} & \forall k = \pi^*, r^* \\ \{1, -5\} & \text{otherwise}, \end{cases} \tag{37}$$

where $\bar{\boldsymbol{\sigma}}^{\pi^*}$ and $\bar{\boldsymbol{\sigma}}^{r^*}$ are extrapolated from the 2-year SPF and Holston et al. (2017)'s measure, respectively. Intuitively, the penalties on equation (37) shrink the estimated parameters toward $\ln \hat{\boldsymbol{\sigma}}^k$, whereby a deviation from these centered values are penalised by a factor λ^k. Our penalty functions assign a great deal of importance to the survey information to the Holston et al. (2017)'s measure of the real rate, as it is highlighted by the values of $\ln \hat{\boldsymbol{\sigma}}^k$, which are relatively small or equal to their extrapolated values, and by the high values assigned to λ^k. For the additional coefficients of the measurement equations, we adopt the following penalty:

$$p(\boldsymbol{\theta}^k) = \lambda^k \left[\boldsymbol{\theta}^k - \bar{\boldsymbol{\theta}}^k\right]^2, \quad \{\lambda^k, \bar{\boldsymbol{\theta}}^k\} = \begin{cases} \{1, 0\} & \forall \theta = \alpha \\ \{\frac{1}{\sqrt{.5}}, 3\} & \theta = \beta \wedge k = \tilde{g} \\ \{\frac{1}{\sqrt{.1}}, 3\} & \theta = \beta \wedge k = r^* \\ \{1, 1\} & \text{otherwise} \end{cases}. \tag{38}$$

Equation (38) centers the parameters α and β around zero and one, implying that we start from the assumption that the information provided by the observed series is unbiased. The only exception is the coefficient $\beta^{\tilde{g}}$, which we center around 3 to acknowledge that the observed value of industrial production might be more volatile than our latent series.

3.2.2 Term structure model

We estimate the parameters of the equation (21) using a quasi-maximum likelihood procedure. Specifically, we fix the parameters $\boldsymbol{\mu}^{\mathbb{P}}$ and $\mathbf{\Phi}^{\mathbb{P}}$ of (18) and we estimate the parameters $\boldsymbol{\mu}^{\mathcal{X}}$, $\mathbf{\Phi}^{\mathcal{X}}$ and $\mathbf{\Sigma}^{\boldsymbol{P}}$ by fitting the term structure of the ILS rates. As in Joslin et al. (2011), the starting point for the estimation of $\mathbf{\Sigma}^{\boldsymbol{P}}$ are the state-space estimates. We maximize the likelihood function by a mixture of simulated annealing and a simplex procedure.

4 Empirical Results

4.1 Expected components and inflation risk premia

This section analyses the decomposition of the two-year ILS rates in EC and IRP. The top panels of Figure 3 report the evolution of the 2 years ILS rates and its EC and

ILS decompositions for the US (panel A) and the EA (panel E). As in Berardi and Plazzi (2018), we find that US short-term expectations are relatively volatile, fluctuating between -44 and 348 bps. The most volatile periods relate to the GFC, the Covid-19 period, and the Ukraine war, reflecting the market's fear of the possibility of a prolonged recession (GFC and early stage of Covid-19) and the fear of high inflation brought about by supply chain bottlenecks, geopolitical tensions and large fiscal stimulus packages (last part of Covid-19 crisis and Ukraine war). In contrast, EA short-term expectations are less volatile, ranging from 74 and 419 bps (265 bps if we exclude the Ukraine war), potentially reflecting the fact that, in contrast to the dual mandate of the FED, the ECB's mandate focuses only on inflation stabilization. As risk premia have been persistently negative between 2013 and 2021, a careful reading of inflation swaps is needed in order to draw firm conclusions regarding the anchoring of inflation expectations in the EA during that period.

Figure 3: 2-Year rates, expected and inflation risk premia components

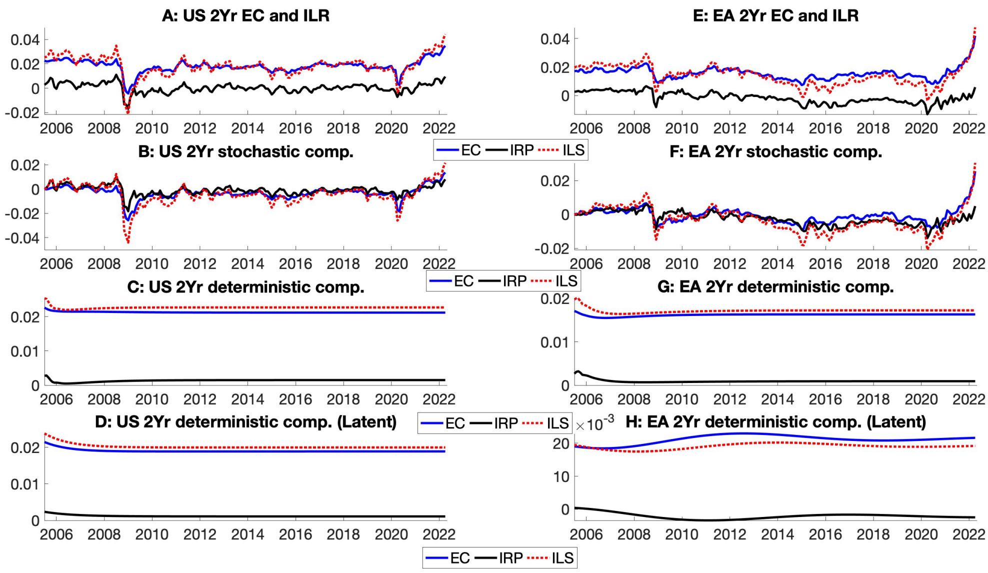

Notes: For the 2-year ILS rates, the Panels of this figure report: (i) Panel A (E): the US (EA) ILS rates, and their decompositions in EC and IRP; (ii) Panel B (F): the decomposition of the stochastic component of the US (EA) rates in EC and IRP; (iii) Panel C (G): the evolution of the deterministic component of the US (EA) rates and its decomposition in EC and IRP; (iv) Panel D (H): the evolution of the deterministic component of the US (EA) rates and its decomposition in EC and IRP for a model without unspanned risk factors and only Level, Slope, and Curvature.

The US inflation risk premium fluctuates between -171 and 110 bps, with the most abrupt changes happening around Lehman's default when it dropped by 181 over four months. It was positive prior to the GFC, a period characterized by relatively stable inflation and growth perspectives, see Figure 2. The deterioration in (expected) economic conditions, associated with the low inflation outlook, contributed to the flip in the sign of the inflation risk premium at the end of 2008. The risk premia fluctuated in the negative territory till the end of 2010. However, in the latter part of the period, negative premia might have been brought about by the post-crisis recovery of the US economy, coupled with the return of inflation to the pre-crisis levels. In the succeeding period, the US inflation risk premia turned negative around the 2010s oil price glut, which was combined with the mini-recession of 2015, and from mid-2019 till the end of 2020, a period characterized first by less-than-expected economic growth and then by the Covid-19 crisis. Our results corroborate the findings of Fleckenstein et al. (2017), Haubrich et al. (2012), and Camba-Mendez and Werner (2017), who suggest that (i) around the GFC and the oil price glut, the probability of deflation might be as high as 30 % for a 2-year horizon (contract), that (ii) the two-year IRP was substantially negative during the GFC, and that (iii) short-term US IRP can be negative for a prolonged period.

The EA inflation risk premium varies between -131 and 67 bps, and it is more persistent than the US counterpart - its first-order autocorrelation is 0.9 against 0.8. It was positive prior to the GFC but turned negative after its inception. In contrast to the US case, EA risk premia did not fall as much and quickly reverted to positive values. Berardi and Plazzi (2018) show that volatility and IRP are negatively related in periods of crisis or market-wide distress. Hence, the quick flip in the sign of EA risk premia is potentially due to the lower volatility of inflation (and its projections) in the region. From the beginning of 2013, risk premia started to decline and turned negative for a prolonged period till the 2022 Russian invasion of Ukraine. This period coincides with the so-called EA lowflation, during which a benign economic recovery coincided with inflation remaining persistently weak and below the ECB's then-prevailing inflation aim (below, but close to, 2% in the medium term) (Stevens and Wauters, 2021). The decline in risk premia intensified around the oil price glut and, after a partial recovery in 2018, reached their lowest levels when the Covid-19 crisis erupted.

Although the EC is the main constituent of ILS rate levels, it is not necessarily the main source of its stochastic variation. Panels B and C (F and G) of Figure 3 depict the evolution of these stochastic and deterministic components for the US (EA), respectively. In both regions, in the absence of shocks, the counterfactual evolution of the ILS rates quickly converges to its mean, conditional on the initial conditions, i.e. 2.27% for the US and 1.70% for the EA, of which more than 95% is linked to the EC components. Noticeably, our model can produce deterministic components of the ILS rates that are not influenced by its low-frequency movements. This is in sharp contrast with the results obtained from a fully-fledged three factors latent model, see panels D and H, whereby for the EA the deterministic components of the ILS rates display oscillating behavior in order to explain a share of the low-frequency variability observed in the data (see Giannone et al., 2019). Turning our attention to the stochastic variations, the bottom panels of Figure 3 underline that a common feature for both regions is that IRP innovations play, to various degrees, an important role in the evolution of stochastic variation of the ILS rates. Remarkably, for the EA the beginning of the lowflation era signs the beginning of a period in which the variation of ILS rates is mostly due to IRP innovations.

Figure A3 in the appendix proposes the decompositions for the 10-year maturity contracts. Overall, the main conclusions of this section hold, namely (i) the inflation risk premium is the main source of variation of the ILS stochastic movements and (ii) for the EA the deterministic component of the models without unspanned risk factor exhibit oscillatory behavior, albeit the fluctuations are less pronounced. In the next section, we investigate in more detail the sources of ILS, IRP, and EC stochastic variation.

4.2 What drives ILS rates?

Variance decomposition

We report the variance decomposition of the 2-year US (EA) ILS rates, its expected and IRP components, and $y_{1,1,t}^{FRP}$, the risk premium in the one-year forward rate in one year, in panels A, B, C, and D of Table 2, respectively. We aggregate the shocks in four groups: (i) Σ_{PCs}, which is the sum of level, slope, and curvature innovations; (ii) Σ_{Gl}, namely the sum of oil and global real activity innovations; (iii) Σ_{Loc} representing the sum of the local macro variable innovations (month-on-month inflation, month-on-month industrial production growth, and one-year risk-free rate); and (iv) the sum of long-term innovations (long-run inflation and real rate trends), labeled Σ_{LR}.

Table 2: Error variance decomposition

US

	A: ILS level				B: Expected component				C: Inflation risk premia				D: Forward risk premia			
Horizon	Σ_{PCs}	Σ_{Gl}	Σ_{Loc}	Σ_{LR}	Σ_{PCs}	Σ_{Gl}	Σ_{Loc}	Σ_{LR}	Σ_{PCs}	Σ_{Gl}	Σ_{Loc}	Σ_{LR}	Σ_{PCs}	Σ_{Gl}	Σ_{Loc}	Σ_{LR}
3M	0.34	0.51	0.15	0.01	0.26	0.51	0.13	0.10	0.32	0.39	0.21	0.08	0.61	0.23	0.08	0.08
12M	0.30	0.49	0.14	0.07	0.23	0.47	0.14	0.16	0.35	0.40	0.17	0.08	0.58	0.25	0.07	0.09
60M	0.23	0.40	0.13	0.25	0.19	0.35	0.11	0.35	0.35	0.38	0.17	0.09	0.58	0.24	0.08	0.10
120M	0.18	0.32	0.11	0.38	0.15	0.27	0.09	0.49	0.35	0.38	0.17	0.09	0.58	0.24	0.08	0.10

EA

	E: ILS level				F: Expected component				G: Inflation risk premia				H: Forward risk premia			
Horizon	Σ_{PCs}	Σ_{Gl}	Σ_{Loc}	Σ_{LR}	Σ_{PCs}	Σ_{Gl}	Σ_{Loc}	Σ_{LR}	Σ_{PCs}	Σ_{Gl}	Σ_{Loc}	Σ_{LR}	Σ_{PCs}	Σ_{Gl}	Σ_{Loc}	Σ_{LR}
3M	0.30	0.38	0.32	0.00	0.17	0.29	0.49	0.06	0.50	0.28	0.17	0.05	0.52	0.28	0.12	0.08
12M	0.32	0.32	0.35	0.01	0.19	0.23	0.43	0.14	0.54	0.24	0.15	0.07	0.59	0.22	0.10	0.09
60M	0.27	0.28	0.35	0.10	0.15	0.17	0.33	0.35	0.51	0.26	0.16	0.07	0.55	0.25	0.13	0.08
120M	0.25	0.26	0.33	0.15	0.13	0.14	0.29	0.44	0.50	0.26	0.16	0.07	0.55	0.25	0.13	0.08

Notes: For a 2-year US (EA) ILS contract panels A to D (E to H) report the error variance decomposition of the ILS rate level, the EC, inflation risk premia, and 1 year forward, respectively. Innovations are grouped as: (i) Σ_{PCs}, which is the sum of level, slope, and curvature innovations; (ii) Σ_{Gl}, namely the sum of oil and global real activity innovations; (iii) Σ_{Loc} representing the sum of the local macro variable innovations (month-on-month inflation, month-on-month industrial production growth, and one-year risk-free rate); and (iv) the sum of long-term innovations (long-run inflation and real rate trends), labeled Σ_{LR}. The error variance decompositions refer to horizons at 3 months (first row), 12 months (second row), 60 months (third row), and 120 months (fourth row).

The variance decomposition reveals that the stochastic variation in ILS rates in both regions is influenced by short-term and long-term economic innovations, with varying contributions depending on the frequency of movements being analyzed. Specifically, two-thirds of high-frequency movements in both areas are related to transitory economic innovations, but the relative contribution of local and international factors differs between regions. In the US, international innovations dominate, accounting for 50% of variations, while only 15% is linked to local economic changes. Conversely, in the EA, the contribution of local and international innovations is evenly distributed, with the importance of international factors decreasing with the forecasting horizon. Additionally, low-frequency movements of ILS rates tend to be less influenced by transitory economic innovations, but again with important regional differences. In the US, transitory economic innovations contribute to one-third of the total variation, while long-term variations increase to 38%. In contrast, in the EA, transitory economic innovations account for 59%, and long-term factors account for 15% of the total variation. Further, a closer examination of the ILS rate decompositions reveals that long-term economic trends primarily impact the low-frequency movement of the EC, while transitory economic innovations are responsible for over 50% of its variations at short horizons. Lastly, we find that the dominant economic innovations behind risk premia variations in both regions are the global ones, accounting for 22 to 40% of the total variation of IRP and FRP. However, a significant portion of the risk-related variation is unexplained by short- and long-term economic innovations, with around one-third (one-half) of US (EA) IRP and more than one-half of FRP in both areas not attributable to economic factors. These findings suggest that factors beyond economic innovations are at play in explaining the variations in the risk component of those contracts. The explanatory power of the various factors for the variance of risk premia is also more stable for risk premia than for the EC.

According to Table A1 listed in the appendix, it is apparent that in the EA, macro factors have a relatively milder effect on the long-term ILS rates. As shown in Figure A3 , a significant fraction of long-term ILS rate variation is linked to IRP movements. And these fluctuations are predominantly driven by innovations in principal component factors. By contrast, in the US, innovations to long-term economic factors appear to hold greater sway over 10-year ILS contracts, with their influence extending both the EC, the IRP, and the 5-year FRP in five years.

Historical decomposition

We analyze the time series evolution of the 2-year US (EA) ILS rates, its expected and IRP components, and $y^{FRP}_{1,1,t}$, the risk premium in the one-year forward rate in one year, in panels A, B, C and D of Figure 4 (Figure 6), respectively. Shock aggregations are similar to the previous section and are summarized in Table 2.

Three periods with high volatility in US rates can be identified from the information presented in panels A to D of Figure 4. The first period, which is characterized by a significant drop in ILS rates, is the post-Lehman era. The second period, spanning from 2014 to 2018, is distinguished by a downward pressure in inflation expectations. Finally, the third period is the (post) Covid-19 era, where ILS rates experienced a sharp decline followed by an increasing trend that continued until the end of the sample. During these three episodes, innovations to international factors played a key role in the stochastic movements of the ILS rates, its EC, and, to a lesser extent, its IRP and FRP components. Specifically, the global slowdown following the GFC and the outburst of the Covid-19 crisis contributed to lower inflation expectations, and, with a more moderate impact, to lower inflation risk premia. For example, over the period September 2008 - May 2009 (March 2020 - June 2020) ILS rates dropped on average by 3.06% (1.96%), with international innovations contributing for 1.81% (1.31%). Over the same period, the EC and the IRP dropped by 2.04% (1.31%) and 1.02% (0.65%), with roughly two-thirds of this variation linked to international innovations.

Figure 4: US: 2-Year ILS, EC, IRP, and 1-year FRP in one year

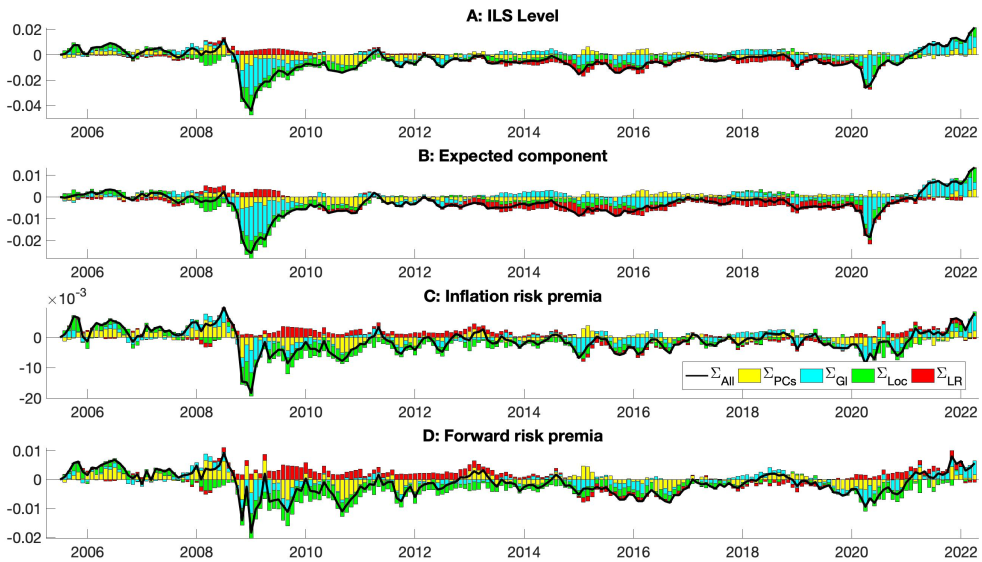

Notes: The historical decomposition is shown of the 2-year US ILS rate (Panel A), its EC (Panel B), its risk premium (Panel C), and its forward risk premium (Panel D). The four groups of innovations, Σ_{PCs}, Σ_{Gl}, Σ_{Loc}, and Σ_{LT}, are described in Table 2.

To gain further insights into the contribution of individual economic innovations on ILS rates movements, Figure 5 reports the detailed historical decompositions for the GFC (left panels), the oil price glut (middle panels) and the Covid-19 era (right panels).[10] From June 2008 to December 2008, the stochastic part of the ILS rates experienced a drop of 565 bp which is equally split between a decrease in the EC (-283 bp) and in the IRP (-282 bp). Negative innovations in oil prices accounted for about 40% of the ILS rate drop, i.e. -241 bp. The other major factors pushing down those rates were the drop in inflation (-113 bp), global demand (-22 bp), and monetary policy (-24bp). Interest rates landed at the zero lower bound at the end of the period but still, they weighed on inflation compensation. The decomposition of ILS rates reveals that, while oil prices and interest rate innovations affected both the EC and the IRP, global demand movements linked mostly to the EC. In the following months, from January 2009 to December 2009, ILS rates bounced back by 370 bp, led mainly by the increase in oil prices (+200 bp) and, to a lesser extent, by the other transitory economic factors. Oil price innovations were the dominant factors during the oil price glut episodes of the mid-2010s. For example, during the first phase of the oil glut, from June 2014 to December 2014, ILS rates dropped by 146 bp (again equally divided between EC and IRP components) and oil price innovations accounted for 40% of this decrease. In the period since 2020, oil price innovations play an important role too. However, inflation innovations have a more persistent upward contribution, in particular via the expectation channel. Albeit small, interest rate innovations push up US inflation swaps, suggesting a relatively slow reaction to the inflation burst by central banks.

[10] Table A2 in the appendix details the major changes' decomposition around these three periods.

Figure 5: US: 2-year ILS, EC, and 1-year FRP in one year

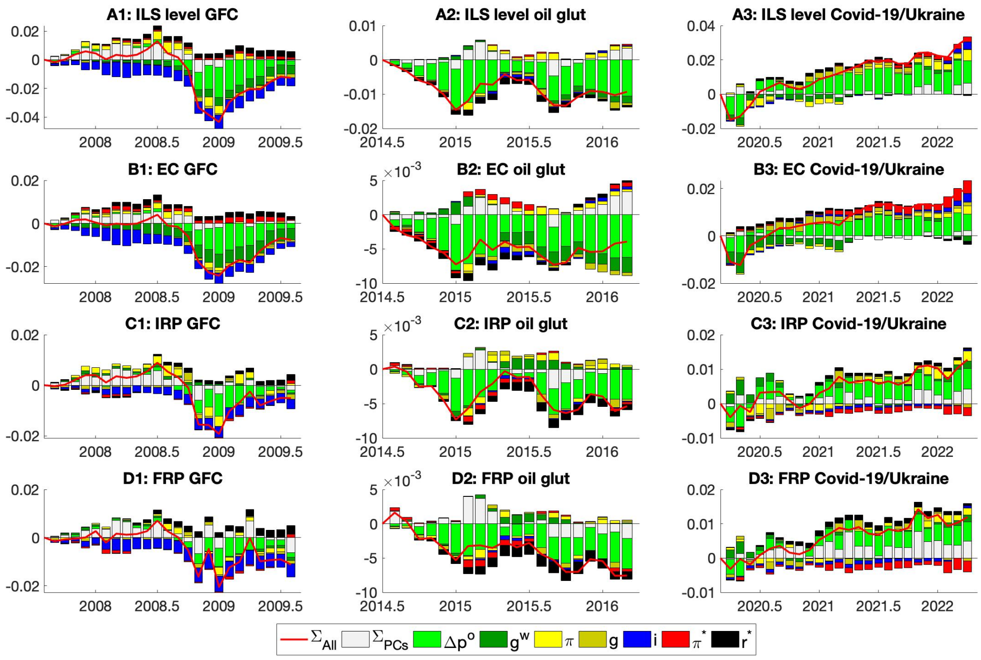

Notes: Panels A1 to D1, A2 to D2, and A3 to D3 depict the historical decomposition of the 2-year US ILS rates, its EC, its inflation risk premium, and its 1-year forward risk premium in one year, respectively, over the GFC, the oil glut, and the Covid-19 and beginning of the Ukrainian war. To ease the readability of the graphs, we group together the innovations of the PCs in Σ_{PCs}. The labels for the other variables follow the notation of Section 2.2, from which we drop the time subscript.

Looking at the EA, Figure 6 indicates that international factors played a significant role in driving ILS movements during the GFC and the oil glut - as is the case for the US. However, there are notable differences between the two regions. To gain a deeper understanding, we focus on the GFC, the oil glut, and the Covid-19 periods, as shown in Figure 7. Here, we can see that PCs and local, transitory, innovations are also pivotal in shaping ILS' stochastic variations. During the GFC, we can infer that for the EA both inflation and interest rates innovations played a more prominent role in the decline of ILS rates. From June to November 2008, ILS rates fell by 275 bp, with 163 bp (roughly 60%) of this decline due to the combined actions of interest rates (mainly via the IRP channel) and inflation (mainly via the EC channel). Moving to the Covid-19 crisis, from October 2020 to March 2022, we can observe that inflation innovation became a dominant component of ILS changes. During this time, we identify three periods characterized by a sharp increase in ILS rates - October 2020 to April 2021, July 2021 to October 2021, and December 2021 to March 2022 - whereby inflation innovations accounted for 65 to 90 bp of a total change of 141 to 203 bp. This influence was mainly through the EC channel, signaling that market participants may have perceived recent increases in inflation to have a lasting impact. However, looking at longer horizons (10 years), Table A3 in the appendix shows that changes in the EC are generally less significant. Since December 2021, we can also see that the 66 bp increase in ILS rates for the EA is mostly due to the combined impact of transitory and permanent inflation innovations (28 bp in total) on the EC channel.

In summary, the historical decomposition reveals the importance of international factors in shaping the dynamics of these rates during various periods. While similarities exist between the US and the EA, there are also key differences, such as the importance of local innovations in shaping the EA market. The analysis also highlights that for short-term maturities (2 years) economic innovations work both through the EC and the IRP channels, pointing out that they are incorporated in marked-based inflation expectation measures, even when they are refined from risk compensation. For longer maturities, the variations in ILS rates are mostly related to the IRP channel, even if we observe that during the recent Covid-19 crisis, the EC channel is becoming more volatile, in part due to the contribution of economic innovations.

Figure 6: EA: 2-year ILS, EC, IRP, and 1-year FRP in one year

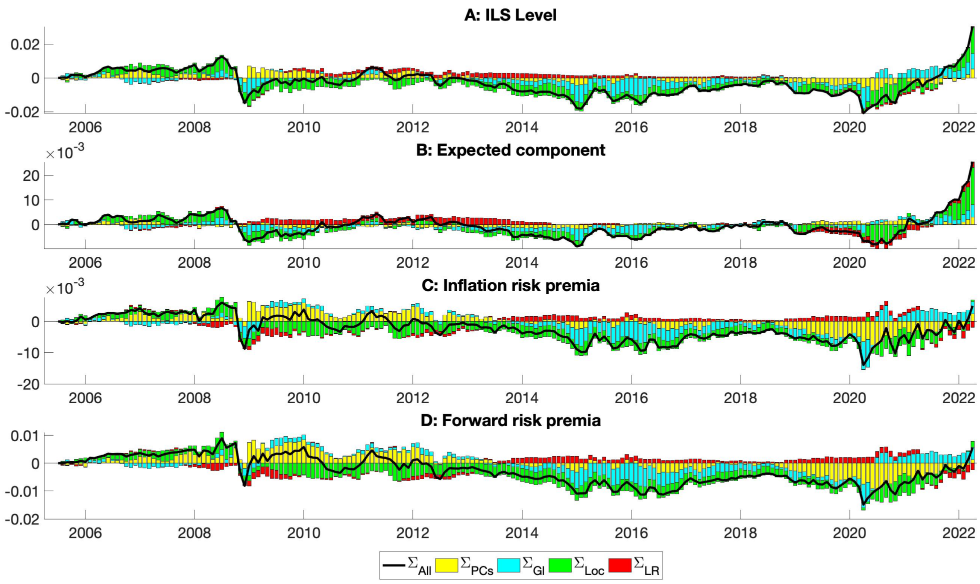

Notes: The historical decomposition is shown of the 2-year EA ILS rate (Panel A), its EC (Panel B), its risk premium (Panel C), and its forward risk premium (Panel D). The four groups of innovations, Σ_{PCs}, Σ_{Gl}, Σ_{Loc}, and Σ_{LT}, are described in Table 2.

Figure 7: EA: 2-year ILS, EC, IRP, and 1-year FRP in one year

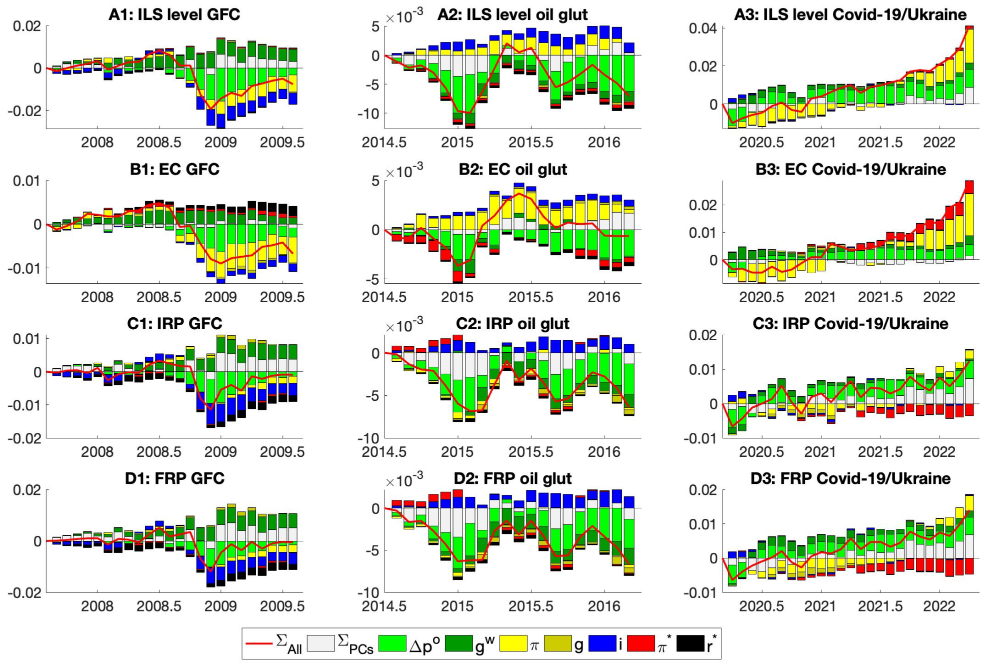

Notes: Panels A1, B1, and C1 (A2, B2, and C2) depict the historical decomposition of the 2-year EA ILS rates, its EC, its inflation risk premium, and its forward risk premium, respectively, over the oil glut (Covid-19 and beginning of the Ukrainian war). To ease the readability of the graphs, we group together the innovations of the PCs in Σ_{PCs}. The labels for the other variables follow the notation of Section 2.2, from which we drop the time subscript.

4.3 Campbell-Shiller tests

In this last subsection, we test the validity of the Expectation Hypothesis (EH) in the government bond market using two types of Campbell and Shiller (1991) regressions. The main goal is to assess if and to what extent the risk measures extracted with our model have theoretical underpinning, i.e. can correct the potential deviation of the EH in the ILS market.

First Campbell-Shiller test. To derive the first test, we consider the ex-post annualized excess returns of entering at time t an n-period ILS contract as the fixed leg counterpart and then closing this position after k years, at t+k, by entering an n-k ILS contract as a floating leg counterpart. We label this quantity $\mathcal{R}^n_{t,t+k}$ and we write it as:

$$\mathcal{R}^n_{t,t+k} = \frac{n}{k} Y_{n,t} - \frac{n-k}{k} Y_{n-k,t+k} - \pi_{\tau,\tau+k}, \tag{39}$$

where $Y_{n,t}$ and $Y_{n-k,t+k}$ are ILS rates, and $\pi_{\tau,\tau+k}$ is the floating payment related to the strategy, i.e. the k-period inflation between the τ and $\tau + k$, and $\tau < t$ accounts for the lagged indexation. Taking the expectations of (39) and replacing $\mathbb{E}_t \pi_{\tau,\tau+k}$ by the k-period ILS rate at time t, we express the expected excess returns as:

$$\mathbb{E}_t \mathcal{R}^n_{t,t+k} = S_{n-k,t} + \frac{n-k}{k}(Y_{n,t} - \mathbb{E}_t Y_{n-k,t+k}), \tag{40}$$

where $S_{n-k,t}$ is the spread between the n- and k-period ILS rate at time t. Rearranging (40) as

$$\mathbb{E}_t Y_{n-k,t+k} - Y_{k,t} = \frac{k}{n-k} S_{n-k,t} - \frac{k}{n-k} \mathbb{E}_t \mathcal{R}^n_{t,t+k}, \tag{41}$$

and by (i) replacing $\mathbb{E}_t \mathcal{R}^n_{t,t+k}$ by the model-implied expected excess return, $\tilde{\mathcal{R}}^n_{t,t+k}$, and by (ii) accounting for the risk premium component in the k-period ILS rate at time t, $y^{tp}_{k,t}$, we derive the following testable equation:

$$Y^{n-k}_{t+k} - Y_{k,t} = \beta^{n,k}_0 + \beta^{n,k}_1 \frac{k}{n-k} S_{n-k,t} - \beta^{n,k}_2 \frac{k}{n-k} (\tilde{\mathcal{R}}^n_{t,t+k} - y^{tp}_{k,t}) + \eta^{n,k}_{t,t+k}. \tag{42}$$

Campbell and Shiller (1991) and subsequent studies have investigated the validity of the Expectation Hypothesis in the government bond market mainly in two by mainly using two approaches: (1) by setting $\beta^{n,k}_2 = 0$ in (42) and testing if $\beta^{n,k}_1 = 1$, i.e. the so-called restricted model; (2) and/or by leaving $\beta^{n,k}_2$ unrestricted and testing if $\beta^{n,k}_1 = 1$ and $\beta^{n,k}_2 = -1$, i.e. the so-called unrestricted model.

The left (right) panels of Table 3 report the slope coefficients related to (42) for the EA (US) market, for a holding period of one year, i.e. $k = 1$, and for 2- to 5-, 7- and 10-year maturities. Panels A report the results for the restricted model, i.e. with $\beta_2 = 0$. The subsequent panels display the slopes for a fully latent model (panels B) and a 6-lag model with macro and world factors (panels F). The table also reports the p-value for the joint hypothesis that $\beta_1 = 1$ and $\beta_2 = -1$ and the Newey-West robust standard errors with automatically selected lags.

The results from the restricted model (panels A) highlight marked differences between the two regions. Specifically, the slope coefficients for the US are more precisely estimated than those of the EA, which are not different from one and whose standard errors increase with maturity. This results in a rejection of the EH in the US but not in the EA. Correcting the regressions with the risk premia obtained from a fully latent three-factor model delivers large positive β_1 coefficients for both regions and large negative β_2 coefficients for short-term US contracts. This leads to a generalized rejection of the joint hypothesis $\beta_1 = 1$ and $\beta_2 = -1$ (with the only exception of the two-year EA contracts), which indicates that inflation risk premia obtained with these models are inconsistent with the theoretical expression (41).

Using our macro-finance model's risk premia in regression (42) delivers divergent results for the two regions. The EA β_1 coefficients increase till the two-year contracts and then decrease for longer maturities. A reverse pattern is observed for the β_2 coefficients, i.e. decreasing till the two-year contracts and then increasing for longer maturities. The F-test p-values reveal that the joint hypothesis $\beta_1 = 1$ and $\beta_2 = -1$ is not rejected for maturities of 7 years or lower. For the US, correcting for risk premia leads to an increase in short-term β_1 coefficients, many of which are statistically different from one. In contrast, β_2 coefficients are all statistically different from -1, with a humped-shaped pattern that is discontinuous across models. The F-test p-values indicate that the joint, theoretical hypothesis, indicated by (41) is rejected at 5% level for all maturities and models, except for long-term contracts (10 years).

Table 3: Campbell-Shiller regressions: first test

EA

A1	Restricted model					
n	1	2	3	5	7	10
β_1	-0.13	0.08	0.11	0.09	-0.12	-0.38
se	0.79	0.78	0.82	0.85	0.98	1.15
B1	$w=0, m=0, p=3, \Upsilon=1$					
n	1	2	3	5	7	10
β_1	1.09	1.78	2.16	2.39	2.56	2.44
se	0.67	0.72	0.83	0.88	1.03	1.23
β_2	-1.79	-1.06	-1.00	-0.99	-0.96	-0.82
se	0.70	0.40	0.35	0.33	0.31	0.29
pval	0.02	0.13	0.01	0.00	0.00	0.00
F1	$w=2, m=3, p=3, \Upsilon=6$					
n	1	2	3	5	7	10
β_1	0.45	0.75	0.74	0.67	0.28	-0.46
se	0.96	0.75	0.74	0.73	0.78	0.91
β_2	-0.99	-1.12	-1.04	-1.04	-1.07	-1.01
se	0.77	0.46	0.38	0.34	0.32	0.31
pval	0.30	0.61	0.75	0.66	0.22	0.01

US

A2	Restricted model					
n	1	2	3	5	7	10
β_1	1.69	1.41	1.62	1.57	1.47	1.46
se	0.42	0.35	0.34	0.39	0.45	0.47
B2	$w=0, m=0, p=3, \Upsilon=1$					
n	1	2	3	5	7	10
β_1	2.22	1.98	2.11	2.02	1.84	1.70
se	0.50	0.39	0.39	0.43	0.48	0.49
β_2	-2.40	-2.03	-1.52	-1.32	-1.08	-0.90
se	0.89	0.53	0.41	0.37	0.29	0.24
pval	0.00	0.00	0.00	0.00	0.01	0.03
F2	$w=2, m=3, p=3, \Upsilon=6$					
n	1	2	3	5	7	10
β_1	2.05	2.35	2.31	2.07	1.62	1.19
se	0.64	0.50	0.40	0.39	0.37	0.36
β_2	-0.48	-1.67	-1.48	-1.48	-1.42	-1.26
se	0.45	0.42	0.37	0.35	0.27	0.23
pval	0.00	0.00	0.00	0.00	0.00	0.10

Notes: The table reports the slope coefficients related to (42) with holding period (k) equal to one year and for 1-, 2-, 3-, 5-, 7-, and 10-year maturities (n). Panels A report the results for the restricted model $\beta_2 = 0$. The subsequent panels display the slopes for the unrestricted models with $\mathbb{E}_t\mathcal{R}^n_{t,t+k}$ obtained via a fully latent model (panels B), and models with only macro and world factors (panels F). The symbols refer to the number of world factors (w), macro variables (m), ILS principal components (p), and model lags (Υ). The table also reports the p-value for the joint hypothesis that $\beta_1 = 1$ and $\beta_2 = -1$.

Second Campbell-Shiller test. The second test derives from (40) as follows. We set $k = 1$ and subtract from both sides the model-implied instantaneous ILS rate (first line below). Subsequently, we substitute the ILS rate in itself (second and third lines):

$$\begin{aligned} Y_{n,t} - Y_{1,t} &= \frac{1}{n}Y_{1,t} + \frac{n-1}{n}\mathbb{E}_t Y^{n-1}_{t+1} + \frac{1}{n}\mathbb{E}_t\mathcal{R}^n_{t,t+1} - Y_{1,t}, \\ &= \frac{1}{n}(Y_{1,t} + \mathbb{E}_t\mathcal{R}^n_{t,t+1}) + \frac{1}{n}\mathbb{E}_t(Y_{1,t+1} + (n-2)\mathbb{E}_t Y^{n-2}_{t+2} + \mathbb{E}_t\mathcal{R}^{n-1}_{t+1,t+2}) - Y_{1,t} \\ &= \frac{1}{n}\sum_{j=0}^{n-1}\mathbb{E}_t Y_{1,t+j} + \frac{1}{n}\sum_{j=0}^{n-1}\mathbb{E}_t\mathcal{R}^n_{t+j,t+j+1} - Y_{1,t} \end{aligned}$$

Rearranging the last expression, we write the difference between the average expected one-month ILS rate and its current value as a function of the ILS slope and the inflation risk premium:

$$\frac{1}{n}\sum_{j=0}^{n-1}\mathbb{E}_t Y_{1,t+j} - Y_{1,t} = Y_{n,t} - Y_{1,t} + \frac{1}{n}\sum_{j=0}^{n-1}\mathbb{E}_t\mathcal{R}^n_{t+j,t+j+1}. \tag{43}$$

By replacing in the latter equation the realized one-month inflation and the model-implied inflation risk premium, we derive the following testable equation:

$$\frac{1}{n}\sum_{j=0}^{n-1}\pi_{\tau+j-1,\tau+j} - Y_{1,t} = \beta^n_0 + \beta^n_1 S_{n-1,t} - \beta^n_2 y^{IRP}_{n,t} + \eta^n_{t,t+n}. \tag{44}$$

where (i) $\pi_{\tau,\tau+1}$ is the *1*-period inflation between the τ and $\tau + k$, with $\tau < t$ to account for the lagged indexation, (ii) $S_{n-1,t}$ is the spread between the n-period ILS rate and its one-period counterpart, and (iii) $y^{IRP}_{n,t}$ is the inflation risk premium on an n-period ILS contract. We rely on (44) to assess the validity of the Expectation Hypothesis in the ILS market and to investigate the reliability of the model-implied inflation risk premia. We first run a restricted version of (44) with $\beta^n_2 = 0$ and, subsequently, we assess if the model-implied inflation risk premia are in line with their theoretical values implied by (43), i.e. $\beta^n_2 = -1$ and $\beta^n_1 = 1$.

The left (right) panels of Table 4 report the slope coefficients related to (44) for the EA (US) market, for 1- to 5-year maturities. The β^n_1 coefficients from the restricted regressions (panels A) indicate a clear rejection of the EH for the US data, where all coefficients are statistically higher than one, independently of the maturity considered. The EA analysis delivers mixed results, with the EH rejected for medium-term maturities, i.e. higher than two years. The unrestricted model delivers slightly different results for the two regions if one adopts the inflation risk premia obtained from a fully latent model. For EA data, both β^n_1 and β^n_2 are inflated upward, leading to coefficients that are statistically different from their theoretical values (except for β^1_1). For the US market, correcting for inflation risk premia has little impact on the slope coefficients, which remain statistically higher than 1, although β^n_2 values are not statistically different from their theoretical values.

In summary, our analysis indicates the presence of a fluctuating risk premium in the ILS market, despite a weaker rejection of the EH compared to the government bond market. The use of our new affine term structure models for risk adjustments appears to generate dependable time-varying risk premium trends, subject to variations in contract maturity, test type, and country/region.

Table 4: Campbell-Shiller regressions: second test

	EA						**US**				
A1	Restricted model					**A2**	Restricted model				
n	1	2	3	4	5	n	1	2	3	4	5
β_1	0.94	1.23	1.38	1.35	1.18	β_1	1.81	1.45	1.30	1.26	1.16
se	0.36	0.14	0.08	0.08	0.08	*se*	0.26	0.09	0.06	0.04	0.05
B1	$w = 0, m = 0, p = 3, \Upsilon = 1$					**B2**	$w = 0, m = 0, p = 3, \Upsilon = 1$				
n	1	2	3	4	5	n	1	2	3	4	5
β_1	1.72	1.77	1.92	1.75	1.43	β_1	1.78	1.47	1.34	1.31	1.20
se	0.44	0.22	0.13	0.07	0.06	*se*	0.28	0.10	0.07	0.04	0.04
β_2	-0.64	-0.49	-0.54	-0.50	-0.48	β_2	-0.68	-1.44	-1.31	-1.34	-1.26
se	0.41	0.16	0.12	0.07	0.06	*se*	1.18	0.58	0.31	0.17	0.17
pval	0.00	0.00	0.00	0.00	0.00	*pval*	0.00	0.00	0.00	0.00	0.00
F1	$w = 2, m = 3, p = 3, \Upsilon = 6$					**F2**	$w = 2, m = 3, p = 3, \Upsilon = 6$				
n	1	2	3	4	5		1	2	3	4	5
β_1	0.81	1.26	1.46	1.43	1.23	β_1	1.07	1.06	1.14	1.15	1.08
se	0.42	0.17	0.10	0.07	0.06	*se*	0.49	0.11	0.07	0.04	0.04
β_2	-0.79	-0.62	-0.61	-0.67	-0.70	β_2	-1.16	-1.67	-1.36	-1.30	-1.36
se	0.49	0.30	0.20	0.12	0.13	*se*	0.92	0.37	0.28	0.18	0.18
pval	0.36	0.00	0.00	0.00	0.00	*pval*	0.58	0.00	0.00	0.00	0.00

Notes: The table reports the slope coefficients related to (44) for 1-, to 5-year maturities (n). Panels A report the results for the restricted model with $\beta_2 = 0$. The subsequent panels display the slopes for the unrestricted models with $y^{tp}_{n,t}$ obtained via a fully latent model (panels B), and models with only macro and world factors (panels F). The symbols refer to the number of world factors (w), macro variables (m), ILS principal components (p), and model lags (Υ). The table also reports the p-value for the joint hypothesis that $\beta_1 = 1$ and $\beta_2 = -1$.

5 Conclusions

Measuring inflation expectations is an important activity for inflation-targeting central banks. Doing so allows them to monitor whether expectations are anchored to their inflation target and steer policy accordingly. One source of information on expectations is inflation-linked swap rates, as quoted on financial markets. These series are available at a high frequency and reflect market activity. However, the series also contains a risk premium component, which implies that they are not a pure measure of inflation expectations.

Our paper proposes a new model to decompose financial market indicators of inflation expectations into genuine inflation expectations and risk premiums. We develop a no-arbitrage term structure model with stochastic endpoints, distinguishing short-term determinants of inflation risk premia from economically-grounded long-run determinants, such as the equilibrium real interest rate and the inflation target.

Our main findings are the following. First, the decomposition of ILS rates in expected component (EC) and inflation risk premium (IRP) underscores that the latter is an important driver of ILS rates' variation, especially for the EA during the lowflation period. Furthermore, by further decomposing these two components in a deterministic and stochastic part (see Giannone et al., 2019), we point out that the EA models based solely on spanned factors might generate an oscillating behavior in the deterministic part of the EC. This problematic feature is absent in our model. Second, we underline the importance of macroeconomic factors in explaining the stochastic evolution of ILS rates and their EC and IRP parts. For example, our variance and the historical decompositions highlight that innovations in unspanned factors account for more than 45 % of the low-frequency movements in IRP. As a result, they are a primary source of returns variation in several historical episodes, like the 2010s oil price glut. Finally, based on the Campbell and Shiller (1991) regressions, we show that a fully-fledged latent factor model without macro variables might not yield theoretically-consistent coefficients. IRP extracted with our macro-finance model mitigate this problem.

A Appendix

TBC.

Figure A1: Long-run inflation and equilibrium real rate

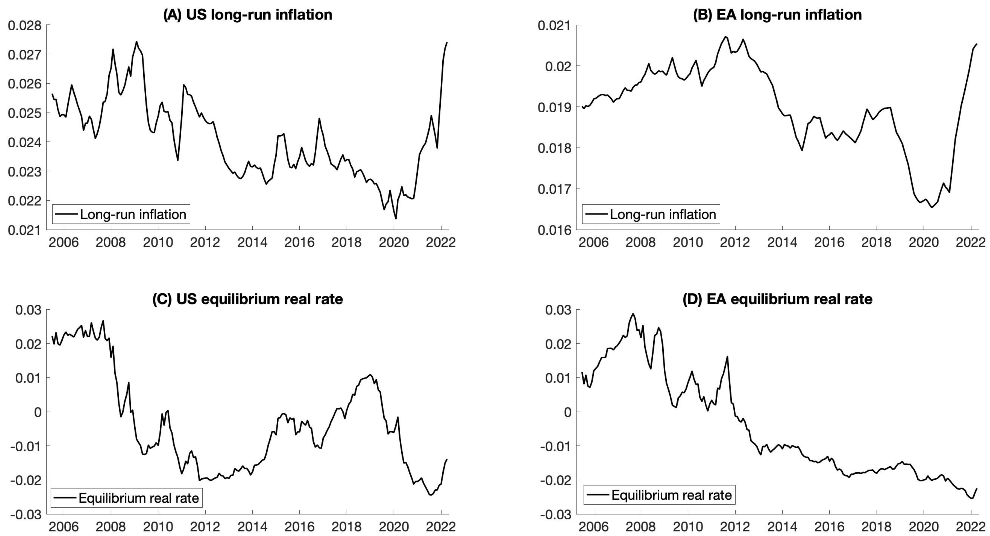

Notes: The top (bottom) panels report the long-run inflation (real rate) for the US and EA, left and right panels, respectively. The estimations refer to a model with six lags.

Figure A2: Fit of measurement equations

(a) Euro area

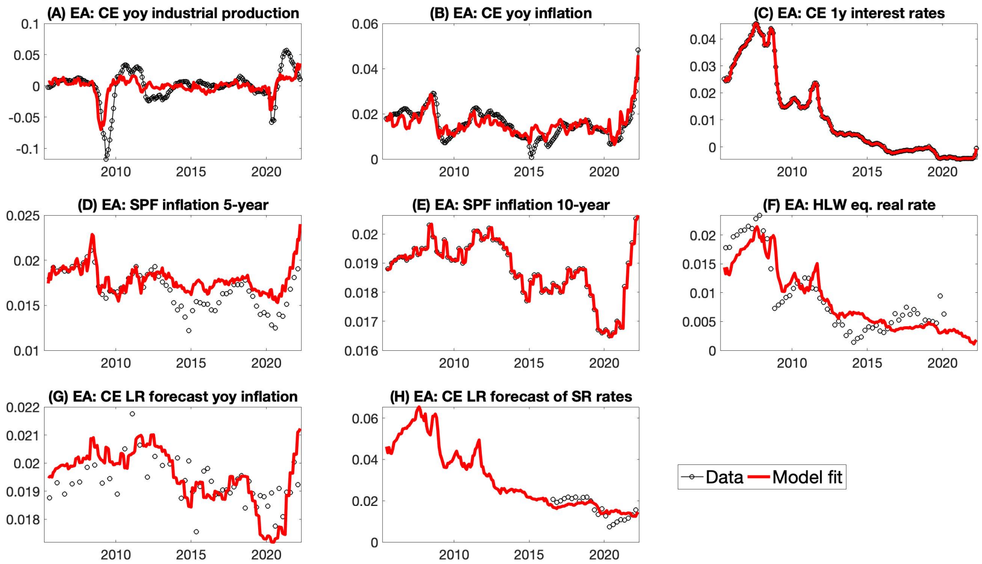

(b) United States

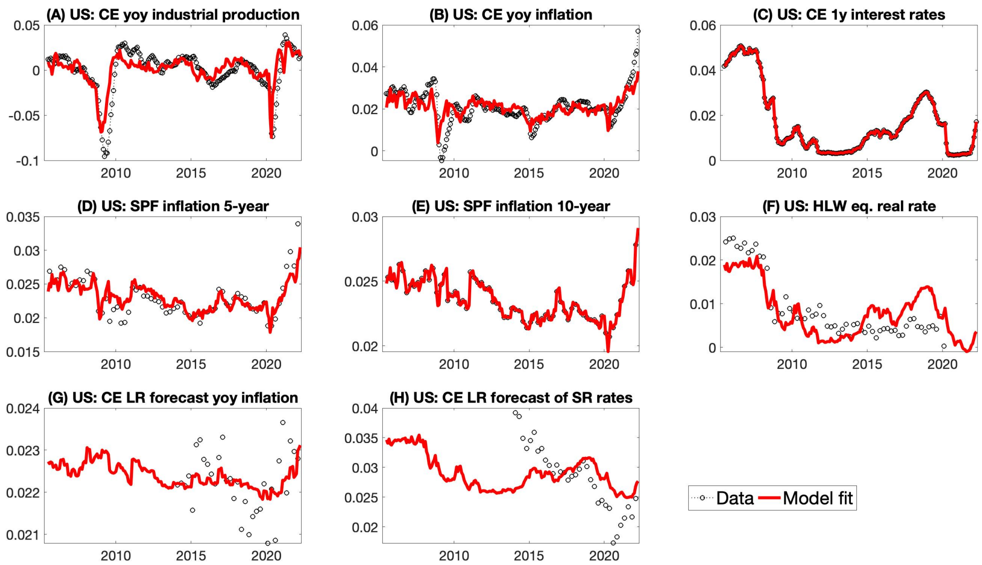

Notes: Model fit is shown for the EA and US in subfigures a and b, respectively. The top panels (A-C) concern, respectively, one-year-ahead Consensus Economics (CE) forecasts of industrial production, inflation, and the one-year risk-free rate. The middle panels concern the quarterly Survey of Professional Forecasters (SPF) forecasts of inflation (panels D and E) and the quarterly Holston et al. (2017) real-rate measure (panel F). The two bottom panels report the model fit for the quarterly long-term CE forecast of inflation (panel G) and the short-term rate (panel H). Each panel depicts the observed data in blue, with circled marks, and uses red lines for the filtered series from a six-lag model with international factors.

Figure A3: 10-year rates, expected and inflation risk premia components

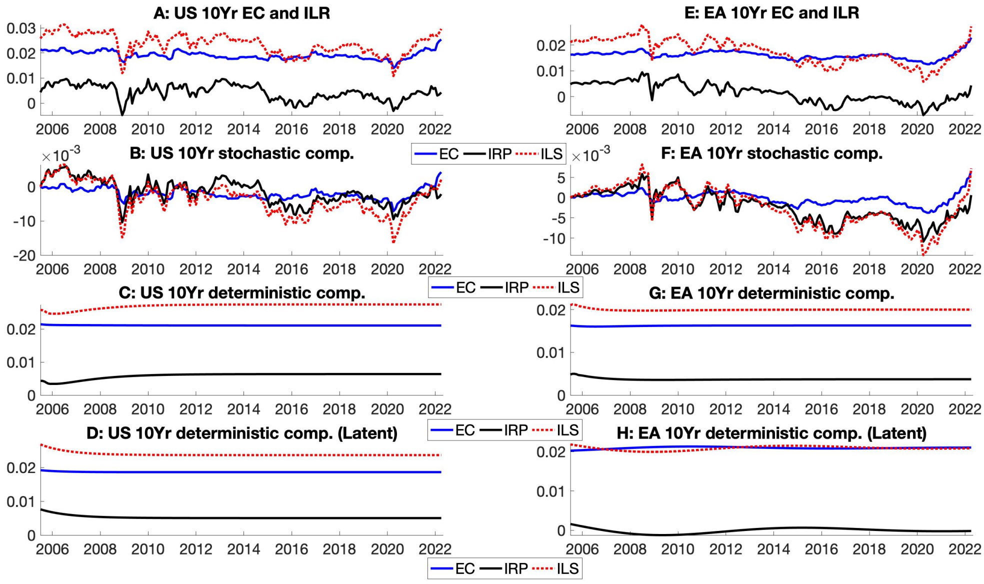

Notes: For the 10-year ILS rates, the Panels of this figure report: (i) Panel A (E): the decomposition of the US (EA) rates in EC and IRP components; (ii) Panel B (F): the decomposition of the stochastic component of the US (EA) rates in EC and IRP; (iii) Panel C (G): the evolution of the deterministic component of the US (EA) rates and its decomposition in EC and IRP; (iv) Panel D (H): the evolution of the deterministic component of the US (EA) rates and its decomposition in EC and IRP for a model without unspanned risk factors and only Level, Slope, and Curvature.

Table A1: Error variance decomposition (10 years)

US

	A: ILS level				B: Expected component				C: Inflation risk premia				D: Forward risk premia			
Horizon	Σ_{PCs}	Σ_{Gl}	Σ_{Loc}	Σ_{LR}	Σ_{PCs}	Σ_{Gl}	Σ_{Loc}	Σ_{LR}	Σ_{PCs}	Σ_{Gl}	Σ_{Loc}	Σ_{LR}	Σ_{PCs}	Σ_{Gl}	Σ_{Loc}	Σ_{LR}
3M	0.48	0.37	0.13	0.02	0.08	0.20	0.05	0.67	0.56	0.20	0.10	0.14	0.71	0.09	0.06	0.14
12M	0.41	0.29	0.14	0.16	0.04	0.11	0.03	0.82	0.53	0.15	0.10	0.22	0.67	0.06	0.07	0.20
60M	0.20	0.14	0.11	0.55	0.01	0.03	0.01	0.96	0.43	0.12	0.15	0.30	0.54	0.05	0.12	0.28
120M	0.12	0.08	0.06	0.73	0.01	0.01	0.00	0.98	0.43	0.12	0.16	0.30	0.54	0.05	0.12	0.28

EA

	E: ILS level				F: Expected component				G: Inflation risk premia				H: Forward risk premia			
Horizon	Σ_{PCs}	Σ_{Gl}	Σ_{Loc}	Σ_{LR}	Σ_{PCs}	Σ_{Gl}	Σ_{Loc}	Σ_{LR}	Σ_{PCs}	Σ_{Gl}	Σ_{Loc}	Σ_{LR}	Σ_{PCs}	Σ_{Gl}	Σ_{Loc}	Σ_{LR}
3M	0.54	0.25	0.21	0.00	0.05	0.13	0.34	0.47	0.65	0.18	0.13	0.05	0.71	0.11	0.12	0.06
12M	0.55	0.25	0.20	0.00	0.04	0.07	0.23	0.66	0.64	0.19	0.12	0.05	0.69	0.14	0.11	0.06
60M	0.49	0.24	0.20	0.08	0.02	0.02	0.07	0.89	0.58	0.22	0.14	0.06	0.65	0.18	0.11	0.06
120M	0.43	0.21	0.17	0.19	0.01	0.01	0.04	0.94	0.58	0.22	0.14	0.06	0.65	0.18	0.11	0.06

Notes: For a 10-year US (EA) ILS contract panels A to D (E to H) report the error variance decomposition of the ILS rate level, the EC, inflation risk premia, and the 5-year in forward risk premium in 5 years, respectively. Innovations are grouped as: (i) Σ_{PCs}, which is the sum of level, slope, and curvature innovations; (ii) Σ_{Gl}, namely the sum of oil and global real activity innovations; (iii) Σ_{Loc} representing the sum of the local macro variable innovations (month-on-month inflation, month-on-month industrial production growth, and one-year risk-free rate); and (iv) the sum of long-term innovations (long-run inflation and real rate trends), labeled Σ_{LR}. The error variance decompositions refer to horizons at 3 months (first row), 12 months (second row), 60 months (third row), and 120 months (fourth row).

Table A2: Detailed historical decomposition: 2-Year ILS

US

Panel A1: Level

GFC	y_2	PCs	Δp^o	g^w	π	g	i	π^*	r^*
2008.06 2008.12	-565	-162	-241	-22	-113	-6	-24	3	0
2008.12 2009.12	370	51	200	19	55	14	42	-8	-4
Oil Glut	y_2	PCs	Δp^o	g^w	π	g	i	π^*	r^*
2014.06 2014.12	-146	-27	-115	11	-2	-1	2	-3	-12
2014.12 2015.04	104	44	80	-13	10	-2	-14	6	-7
2015.04 2015.09	-91	-35	-48	-10	-7	-2	8	-1	4
Covid-19	y_2	PCs	Δp^o	g^w	π	g	i	π^*	r^*
2019.12 2020.03	-207	-9	-164	-16	24	-15	-23	-4	-1
2020.03 2020.08	217	38	158	0	-6	14	-2	1	13
2020.10 2021.06	168	13	106	30	26	-5	-7	9	-4
2021.08 2021.11	66	53	-28	20	39	-13	-1	2	-5
2022.01 2022.03	101	46	28	-20	16	-8	39	13	-12

Panel B1: EC

GFC	y_2^{EC}	PCs	Δp^o	g^w	π	g	i	π^*	r^*
2008.06 2008.12	-283	-72	-138	-12	-42	-14	-5	5	-5
2008.12 2009.12	201	9	116	42	12	18	32	-16	-13
Oil Glut	y_2^{EC}	PCs	Δp^o	g^w	π	g	i	π^*	r^*
2014.06 2014.12	-73	-14	-67	18	-1	0	2	-4	-7
2014.12 2015.04	33	30	41	-30	0	-8	-10	13	-2
2015.04 2015.09	-31	-14	-20	-9	2	6	6	-9	7
Covid-19	y_2^{EC}	PCs	Δp^o	g^w	π	g	i	π^*	r^*
2019.12 2020.03	-143	-1	-92	-40	8	8	-15	-9	-2
2020.03 2020.08	143	9	86	15	-5	24	0	6	7
2020.10 2021.06	85	9	59	18	11	-17	-2	17	-8
2021.08 2021.11	10	25	-20	11	14	-7	0	-6	-7
2022.01 2022.03	76	29	8	-36	16	11	28	28	-8

Panel C1: IRP

GFC	y_2^{IRP}	PCs	Δp^o	g^w	π	g	i	π^*	r^*
2008.06 2008.12	-282	-90	-103	-10	-71	7	-19	-2	5
2008.12 2009.12	168	42	84	-24	42	-4	10	8	9
Oil Glut	y_2^{IRP}	PCs	Δp^o	g^w	π	g	i	π^*	r^*
2014.06 2014.12	-73	-13	-48	-7	-1	0	0	1	-5
2014.12 2015.04	70	14	39	16	10	6	-4	-7	-4
2015.04 2015.09	-61	-21	-28	-1	-9	-8	2	8	-2
Covid-19	y_2^{IRP}	PCs	Δp^o	g^w	π	g	i	π^*	r^*
2019.12 2020.03	-65	-8	-72	24	16	-23	-8	5	1
2020.03 2020.08	74	29	72	-15	-1	-9	-2	-5	6
2020.10 2021.06	83	4	47	12	15	12	-5	-7	4
2021.08 2021.11	56	28	-9	9	25	-6	-1	8	2
2022.01 2022.03	25	17	19	16	0	-20	11	-15	-3

Panel D1: 1-Year/1-Year FRP

GFC	$y_{1,1}^{FRP}$	PCs	Δp^o	g^w	π	g	i	π^*	r^*
2008.06 2008.12	-276	-111	-91	-11	-39	-3	-24	-3	6
2008.12 2009.12	188	67	75	-18	29	3	14	11	8
Oil Glut	$y_{1,1}^{FRP}$	PCs	Δp^o	g^w	π	g	i	π^*	r^*
2014.06 2014.12	-53	2	-43	-4	-2	0	1	1	-9
2014.12 2015.04	27	-7	30	14	11	2	-6	-9	-6
2015.04 2015.09	-44	-15	-25	-4	-3	-9	3	10	-1
Covid-19	$y_{1,1}^{FRP}$	PCs	Δp^o	g^w	π	g	i	π^*	r^*
2019.12 2020.03	-62	-3	-66	21	8	-18	-11	7	2
2020.03 2020.08	68	31	61	-18	-4	-1	-4	-6	10
2020.10 2021.06	60	-1	49	8	6	10	-6	-10	4
2021.08 2021.11	38	18	-10	6	12	3	-1	11	0
2022.01 2022.03	-7	-1	8	14	-6	-12	17	-20	-6

EA

Panel A2: Level

GFC	y_2	PCs	Δp^o	g^w	π	g	i	π^*	r^*
2008.06 2008.11	-275	-30	-123	21	-58	2	-95	0	8
2008.11 2009.12	145	67	93	-33	-10	-3	14	1	17
Oil Glut	y_2	PCs	Δp^o	g^w	π	g	i	π^*	r^*
2014.06 2015.01	-99	-33	-67	-18	11	0	16	-4	-4
2015.01 2015.04	120	45	71	5	9	-1	-9	1	-1
2015.04 2015.08	-76	-40	-53	6	-4	1	14	0	0
Covid-19	y_2	PCs	Δp^o	g^w	π	g	i	π^*	r^*
2019.12 2020.03	-137	-27	-118	9	-13	-7	19	-1	2
2020.03 2020.08	109	27	149	29	-69	-2	-25	-2	1
2020.10 2021.04	141	8	57	3	65	5	5	-1	-1
2021.08 2021.11	98	32	-29	2	85	-4	6	5	1
2019.12 2022.03	203	57	27	18	90	3	2	4	2

Panel B2: EC

GFC	y_2^{EC}	PCs	Δp^o	g^w	π	g	i	π^*	r^*
2008.06 2008.11	-128	-1	-49	-2	-61	-2	-11	-3	0
2008.11 2009.12	20	-7	33	-26	18	1	-14	-1	15
Oil Glut	y_2^{EC}	PCs	Δp^o	g^w	π	g	i	π^*	r^*
2014.06 2015.01	-31	-5	-26	-14	14	0	4	-3	-2
2015.01 2015.04	61	16	23	14	4	1	0	3	0
2015.04 2015.08	-28	-14	-17	4	-3	1	2	0	-1
Covid-19	y_2^{EC}	PCs	Δp^o	g^w	π	g	i	π^*	r^*
2019.12 2020.03	-39	-5	-49	22	-13	2	2	1	0
2020.03 2020.08	-9	7	52	-13	-58	4	-1	0	0
2020.10 2021.04	47	-12	21	1	38	-1	1	-3	0
2021.08 2021.11	51	5	-9	-8	56	-2	0	8	1
2019.12 2022.03	155	27	8	26	85	-1	0	11	-1

Panel C2: IRP

GFC	y_2^{IRP}	PCs	Δp^o	g^w	π	g	i	π^*	r^*
2008.06 2008.11	-148	-29	-75	23	3	4	-84	3	7
2008.11 2009.12	125	74	59	-7	-28	-5	27	2	2
Oil Glut	y_2^{IRP}	PCs	Δp^o	g^w	π	g	i	π^*	r^*
2014.06 2015.01	-68	-28	-41	-4	-3	-1	13	-1	-3
2015.01 2015.04	59	29	48	-9	4	-2	-9	-2	-1
2015.04 2015.08	-48	-26	-36	2	-1	0	12	0	1
Covid-19	y_2^{IRP}	PCs	Δp^o	g^w	π	g	i	π^*	r^*
2019.12 2020.03	-98	-22	-68	-14	-1	-10	17	-2	1
2020.03 2020.08	118	20	97	42	-11	-6	-24	-2	2
2020.10 2021.04	94	20	35	1	27	5	5	2	-1
2021.08 2021.11	47	27	-20	10	29	-2	6	-3	-1
2019.12 2022.03	48	31	18	-8	4	5	2	-7	3

Panel D2: 1-Year/1-Year FRP

GFC	$y_{1,1}^{FRP}$	PCs	Δp^o	g^w	π	g	i	π^*	r^*
2008.06 2008.11	-171	-47	-72	24	-10	4	-81	4	7
2008.11 2009.12	139	102	55	-10	-25	-6	15	3	6
Oil Glut	$y_{1,1}^{FRP}$	PCs	Δp^o	g^w	π	g	i	π^*	r^*
2014.06 2015.01	-62	-18	-39	-10	-3	-2	13	0	-3
2015.01 2015.04	47	24	43	-10	3	-1	-8	-3	-1
2015.04 2015.08	-42	-31	-31	5	1	1	12	-1	1
Covid-19	$y_{1,1}^{FRP}$	PCs	Δp^o	g^w	π	g	i	π^*	r^*
2019.12 2020.03	-94	-23	-70	-7	-2	-8	16	-2	2
2020.03 2020.08	85	13	88	36	-22	-8	-22	-2	2
2020.10 2021.04	85	32	29	-5	15	8	4	2	-2
2021.08 2021.11	42	27	-17	7	27	-1	5	-6	-1
2019.12 2022.03	65	24	17	-1	26	2	2	-9	4

Notes: For a 2-year US (EA) ILS contract the second column of panels A1 to D1 (A2 to D2) report the changes in the stochastic part of the ILS rate level (y_2), the EC (y_2^{EC}), inflation risk premia (y_2^{IRP}), and the 1-year in forward risk premium in one year ($y_{1,1}^{FRP}$), respectively. The first columns report the time periods when the changes are computed, while the third columns report the total changes of the PCs. The remaining columns list the changes in the other variables, which are labelled following the notation of Section 2.2. We drop the time subscript to ease the notation.

Table A3: Detailed historical decomposition: 10-Year ILS

US

Panel A1: Level

GFC	y_2	PCs	Δp^o	g^w	π	g	i	π^*	r^*
2008.06 2008.12	-167	-25	-88	-7	-34	-1	-21	3	6
2008.12 2009.12	149	36	73	4	17	3	11	-4	8
Oil Glut	y_2	PCs	Δp^o	g^w	π	g	i	π^*	r^*
2014.06 2014.12	-67	-13	-42	2	-1	-0	2	-3	-13
2014.12 2015.04	15	-3	27	-2	3	2	-7	4	-9
2015.04 2015.09	-45	-20	-16	-3	-4	-4	4	-1	-1
Covid-19	y_2	PCs	Δp^o	g^w	π	g	i	π^*	r^*
2019.12 2020.03	-86	-17	-58	0	8	-6	-14	-3	2
2020.03 2020.08	93	32	57	-4	0	-3	-5	0	15
2020.10 2021.06	60	-2	40	9	8	2	-7	6	4
2021.08 2021.11	18	17	-12	5	14	-3	-1	2	-3
2022.01 2022.03	23	-1	8	-4	4	-5	20	9	-9

Panel B1: EC

GFC	y_2^{EC}	PCs	Δp^o	g^w	π	g	i	π^*	r^*
2008.06 2008.12	-55	-15	-29	-3	-9	-3	-1	6	-1
2008.12 2009.12	28	2	24	9	3	4	7	-18	-3
Oil Glut	y_2^{EC}	PCs	Δp^o	g^w	π	g	i	π^*	r^*
2014.06 2014.12	-18	-3	-14	4	-0	-0	0	-4	-1
2014.12 2015.04	19	6	8	-7	-0	-2	-2	15	-0
2015.04 2015.09	-16	-3	-4	-2	0	1	1	-12	1
Covid-19	y_2^{EC}	PCs	Δp^o	g^w	π	g	i	π^*	r^*
2019.12 2020.03	-38	0	-19	-9	2	2	-3	-10	-1
2020.03 2020.08	36	2	18	4	-1	5	0	8	1
2020.10 2021.06	33	2	12	4	2	-4	-0	18	-2
2021.08 2021.11	-6	5	-4	2	3	-1	0	-9	-1
2022.01 2022.03	42	6	2	-8	3	3	6	32	-1

Panel C1: IRP

GFC	y_2^{IRP}	PCs	Δp^o	g^w	π	g	i	π^*	r^*
2008.06 2008.12	-113	-10	-59	-4	-26	2	-21	-3	7
2008.12 2009.12	121	34	49	-5	15	-1	5	14	11
Oil Glut	y_2^{IRP}	PCs	Δp^o	g^w	π	g	i	π^*	r^*
2014.06 2014.12	-49	-10	-28	-2	-1	-0	1	1	-12
2014.12 2015.04	-4	-10	18	5	3	4	-5	-11	-8
2015.04 2015.09	-28	-17	-12	-1	-4	-5	2	11	-2
Covid-19	y_2^{IRP}	PCs	Δp^o	g^w	π	g	i	π^*	r^*
2019.12 2020.03	-48	-17	-39	9	7	-8	-11	7	3
2020.03 2020.08	56	31	40	-7	1	-8	-6	-7	14
2020.10 2021.06	27	-4	28	6	5	6	-7	-12	6
2021.08 2021.11	24	12	-8	2	11	-2	-1	11	-1
2022.01 2022.03	-19	-7	6	4	1	-7	15	-23	-7

Panel D1: 5-Year/5-Year FRP

GFC	$y_{1,1}^{FRP}$	PCs	Δp^o	g^w	π	g	i	π^*	r^*
2008.06 2008.12	-42	32	-47	-2	-15	4	-19	-4	8
2008.12 2009.12	96	23	39	1	5	-1	0	16	13
Oil Glut	$y_{1,1}^{FRP}$	PCs	Δp^o	g^w	π	g	i	π^*	r^*
2014.06 2014.12	-48	-15	-22	-0	0	-0	2	1	-13
2014.12 2015.04	-21	-13	13	2	-0	5	-5	-13	-9
2015.04 2015.09	-22	-19	-6	-1	-4	-3	2	12	-2
Covid-19	$y_{1,1}^{FRP}$	PCs	Δp^o	g^w	π	g	i	π^*	r^*
2019.12 2020.03	-43	-23	-28	5	5	-2	-11	8	3
2020.03 2020.08	51	32	31	-5	3	-10	-7	-8	16
2020.10 2021.06	11	-6	20	4	4	4	-7	-14	7
2021.08 2021.11	16	10	-8	-0	9	-3	-2	12	-2
2022.01 2022.03	-27	-11	4	-0	4	-4	14	-26	-8

EA

Panel A2: Level

GFC	y_2	PCs	Δp^o	g^w	π	g	i	π^*	r^*
2008.06 2008.11	-140	-29	-54	17	-21	3	-61	1	3
2008.11 2009.12	102	77	39	-7	-8	-4	-1	1	3
Oil Glut	y_2	PCs	Δp^o	g^w	π	g	i	π^*	r^*
2014.06 2015.01	-53	-21	-29	-9	1	-0	10	-4	-1
2015.01 2015.04	30	15	28	-6	2	-2	-6	-1	-0
2015.04 2015.08	-22	-15	-18	3	0	-1	9	-1	0
Covid-19	y_2	PCs	Δp^o	g^w	π	g	i	π^*	r^*
2019.12 2020.03	-62	-17	-47	1	-5	-5	12	-1	0
2020.03 2020.08	46	12	60	20	-25	-6	-13	-2	0
2020.10 2021.04	63	28	23	-2	13	3	1	-1	-0
2021.08 2021.11	46	21	-13	4	25	2	4	3	-0
2019.12 2022.03	66	9	11	3	36	2	1	3	1

Panel B2: EC

GFC	y_2^{EC}	PCs	Δp^o	g^w	π	g	i	π^*	r^*
2008.06 2008.11	-32	1	-11	-1	-12	-1	-5	-3	-0
2008.11 2009.12	2	-4	7	-5	4	1	-4	-1	4
Oil Glut	y_2^{EC}	PCs	Δp^o	g^w	π	g	i	π^*	r^*
2014.06 2015.01	-7	-0	-6	-2	3	0	1	-3	-0
2015.01 2015.04	14	3	5	3	1	0	-0	2	0
2015.04 2015.08	-6	-3	-4	1	-1	0	1	-0	-0
Covid-19	y_2^{EC}	PCs	Δp^o	g^w	π	g	i	π^*	r^*
2019.12 2020.03	-7	-1	-11	4	-3	1	1	1	-0
2020.03 2020.08	-2	1	11	-2	-12	1	-1	-0	-0
2020.10 2021.04	6	-3	5	0	8	-0	-0	-4	0
2021.08 2021.11	16	0	-2	-1	11	-1	0	7	1
2019.12 2022.03	39	5	2	5	17	-0	-0	11	-1

Panel C2: IRP

GFC	y_2^{IRP}	PCs	Δp^o	g^w	π	g	i	π^*	r^*
2008.06 2008.11	-108	-29	-43	17	-9	4	-56	4	4
2008.11 2009.12	100	80	32	-2	-12	-4	3	3	-1
Oil Glut	y_2^{IRP}	PCs	Δp^o	g^w	π	g	i	π^*	r^*
2014.06 2015.01	-46	-21	-23	-7	-2	-1	9	-1	-1
2015.01 2015.04	17	12	23	-9	1	-2	-6	-3	-0
2015.04 2015.08	-16	-12	-15	2	1	-1	8	-0	0
Covid-19	y_2^{IRP}	PCs	Δp^o	g^w	π	g	i	π^*	r^*
2019.12 2020.03	-55	-17	-37	-3	-2	-6	11	-2	0
2020.03 2020.08	48	11	49	22	-13	-7	-13	-2	1
2020.10 2021.04	58	31	18	-3	6	3	1	2	-1
2021.08 2021.11	30	20	-11	5	14	2	4	-4	-1
2019.12 2022.03	27	3	10	-1	19	2	1	-8	1

Panel D2: 5-Year/5-Year FRP

GFC	$y_{1,1}^{FRP}$	PCs	Δp^o	g^w	π	g	i	π^*	r^*
2008.06 2008.11	-79	-19	-32	14	-12	4	-40	4	2
2008.11 2009.12	85	69	24	2	-3	-4	-1	3	-5
Oil Glut	$y_{1,1}^{FRP}$	PCs	Δp^o	g^w	π	g	i	π^*	r^*
2014.06 2015.01	-44	-26	-17	-6	-0	0	7	-1	0
2015.01 2015.04	4	8	15	-8	0	-3	-4	-3	-0
2015.04 2015.08	-4	-3	-7	1	0	-2	6	-0	0
Covid-19	$y_{1,1}^{FRP}$	PCs	Δp^o	g^w	π	g	i	π^*	r^*
2019.12 2020.03	-41	-15	-23	-0	-3	-5	8	-2	-0
2020.03 2020.08	30	13	33	14	-13	-7	-7	-2	0
2020.10 2021.04	46	30	14	-2	2	1	-1	3	-0
2021.08 2021.11	27	19	-9	4	10	4	3	-3	-1
2019.12 2022.03	16	-5	6	-1	20	2	0	-7	0

Notes: For a 10-year US (EA) ILS contract the second column of panels A1 to D1 (A2 to D2) report the changes in the stochastic part of the ILS rate level (y_2), the EC (y_2^{EC}), inflation risk premia (y_2^{IRP}), and the 5-year in forward risk premium in five years ($y_{5,5}^{FRP}$), respectively. The first columns report the time periods when the changes are computed, while the third columns report the total changes of the PCs. The remaining columns list the changes in the other variables, which are labelled following the notation of Section 2.2. We drop the time subscript to ease the notation.

Figure A4: US: 10-year ILS, EC, IRP, and 5-year FRP in five years

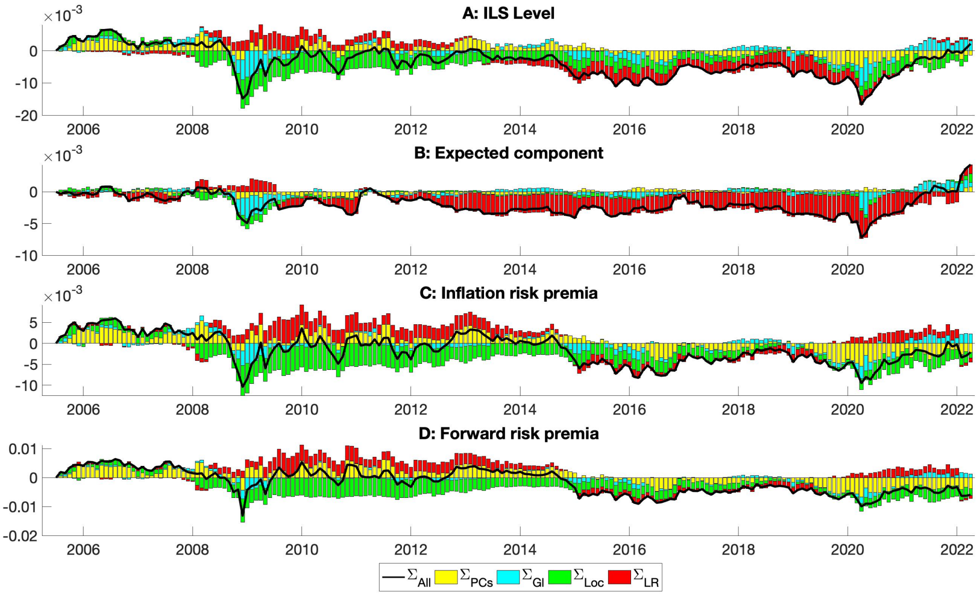

Notes: The historical decomposition is shown of the 10-year US ILS rate (Panel A), its EC (Panel B), its risk premium (Panel C), and the 5-year in forward risk premium in five years (Panel D). The four groups of innovations, Σ_{PCs}, Σ_{Gl}, Σ_{Loc}, and Σ_{LT}, are described in Table 2.

Figure A5: EA: 10-Year ILS, EC, IRP, and 5-year FRP in five years

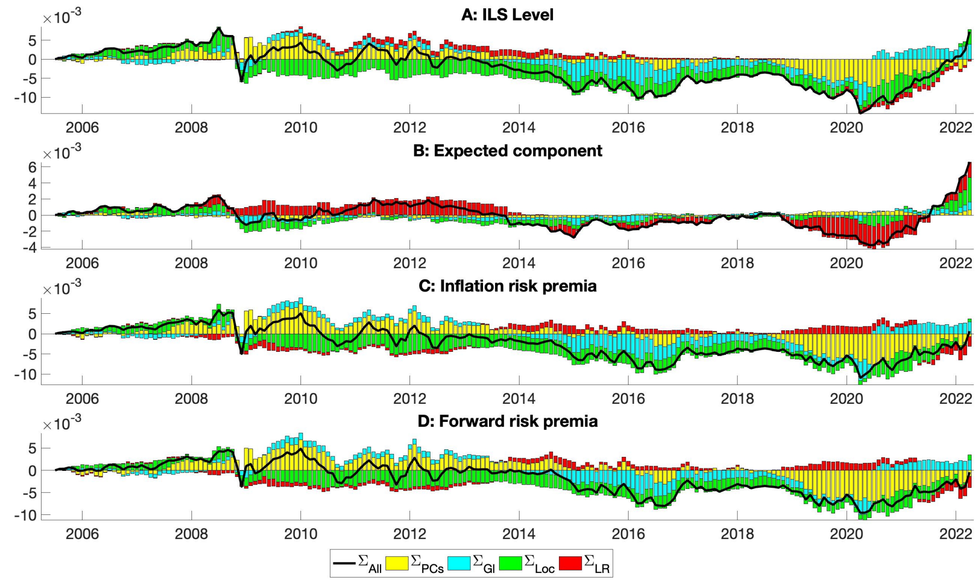

Notes: The historical decomposition is shown of the 10-Year EA ILS rate (Panel A), its EC (Panel B), its risk premium (Panel C), and the 5-year in forward risk premium in five years (Panel D). The four groups of innovations, Σ_{PCs}, Σ_{Gl}, Σ_{Loc}, and Σ_{LT}, are described in Table 2.

Figure A6: US: 10-Year ILS, EC, IRP, and 5-year FRP in five years

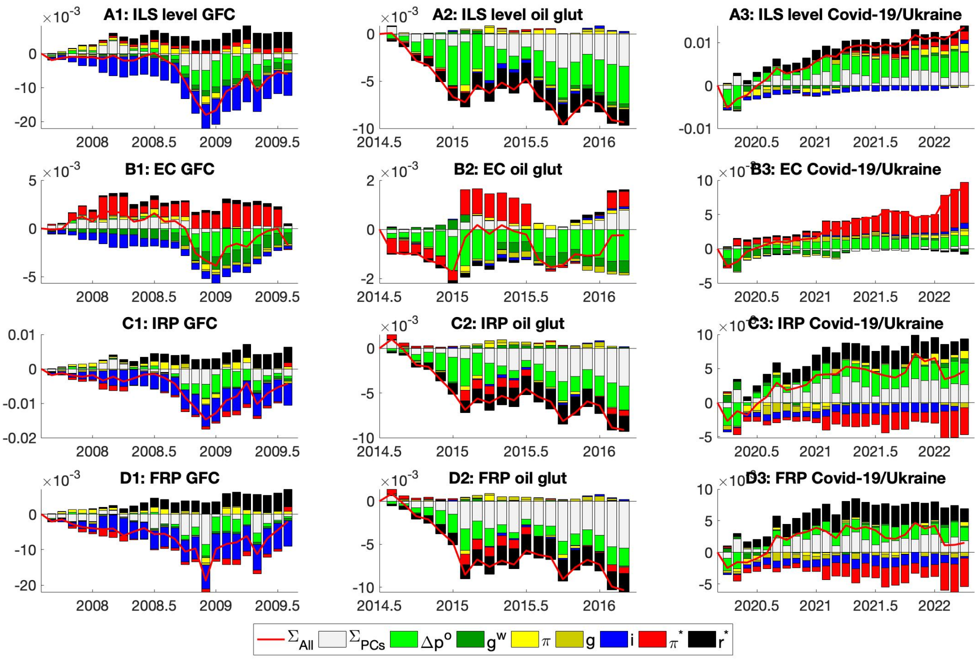

Notes: Panels A1, B1, and C1 (A2, B2, and C2) depict the historical decomposition of the 10-year US ILS rates, its EC, its inflation risk premium, and the 5-year in forward risk premium in five years, respectively, over the oil glut (Covid-19 and beginning of the Ukrainian war). To ease the readability of the graphs, we group together the innovations of the PCs in Σ_{PCs}. The labels for the other variables follow the notation of Section 2.2, from which we drop the time subscript.

Figure A7: EA: 10-Year ILS, EC, IRP, and 5-year FRP in five years

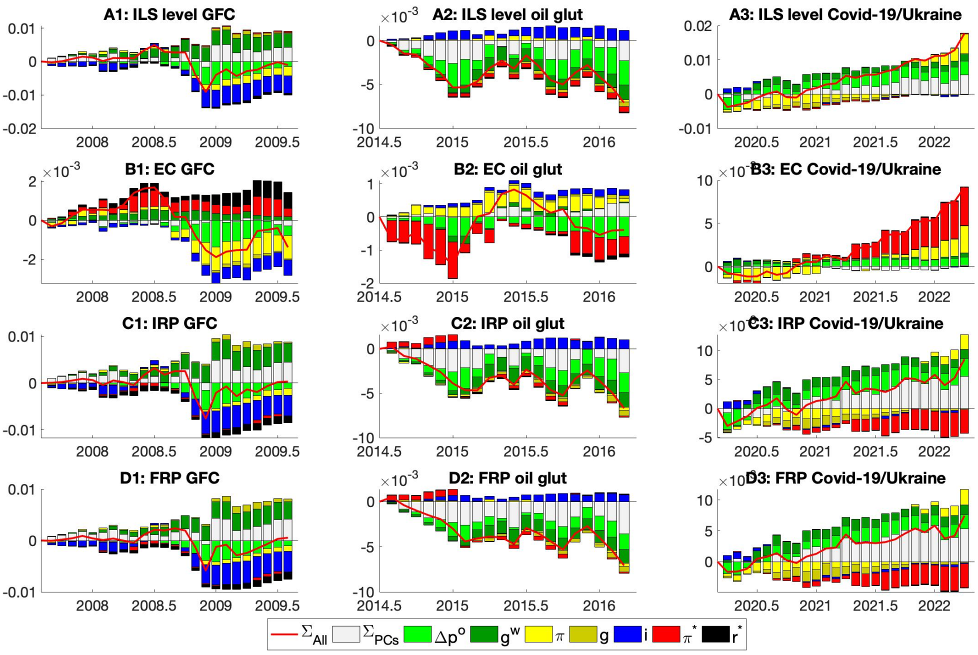

Notes: Panels A1, B1, and C1 (A2, B2, and C2) depict the historical decomposition of the 10-year EA ILS rates, its EC, its inflation risk premium, and the 5-year in forward risk premium in five years, respectively, over the oil glut (Covid-19 and beginning of the Ukrainian war). To ease the readability of the graphs, we group together the innovations of the PCs in Σ_{PCs}. The labels for the other variables follow the notation of Section 2.2, from which we drop the time subscript.

References

Abrahams, M., T. Adrian, R. Crump, E. Moench, and R. Yu (2016). Decomposing real and nominal yield curves. *Journal of Monetary Economics 84*(C), 182–200.

Ang, A., G. Bekaert, and M. Wei (2008). The term structure of real rates and expected inflation. *Journal of Finance 63*(2), 797–849.

Ang, A. and M. Piazzesi (2003). A no-arbitrage vector autoregression of term structure dynamics with macroeconomic and latent variables. *Journal of Monetary Economics 50*(4), 745–787.

Bauer, M. D. and G. D. Rudebusch (2020, May). Interest rates under falling stars. *American Economic Review 110*(5), 1316–54.

Baumeister, C., D. Korobilis, and T. K. Lee (2022, 07). Energy Markets and Global Economic Conditions. *The Review of Economics and Statistics 104*(4), 828–844.

Berardi, A. and A. Plazzi (2018, 02). Inflation Risk Premia, Yield Volatility, and Macro Factors. *Journal of Financial Econometrics 17*(3), 397–431.

Camba-Mendez, G. and T. Werner (2017). The inflation risk premium in the post-lehman period. Working Paper Series 2033, European Central Bank.

Campbell, J. Y. and R. J. Shiller (1991). Yield spreads and interest rate movements: A bird's eye view. *The Review of Economic Studies 58*(3), 495–514.

Carriero, A., S. Mouabbi, and E. Vangelista (2018). Uk term structure decompositions at the zero lower bound. *Journal of Applied Econometrics 33*(5), 643–661.

Christensen, J., J. Lopez, and G. Rudebusch (2010). Inflation expectations and risk premiums in an arbitrage-free model of nominal and real bond yields. *Journal of Money, Credit and Banking 42*(s1), 143–178.

Dewachter, H. and L. Iania (2011). An extended macro-finance model with financial factors. *Journal of Financial and Quantitative Analysis 46*(6), 1893?1916.

Dovern, J., U. Fritsche, and J. Slacalek (2012). Disagreement among forecasters in g7 countries. *The Review of Economics and Statistics 94*(4), 1081–1096.

Fan, J. and R. Li (2001). Variable selection via nonconcave penalized likelihood and its oracle properties. *Journal of the American Statistical Association 96*(456), 1348–1360.

Fisher, I. (1896). Appreciation and interest: A study of the influence of monetary appreciation and depreciation on the rate of interest with applications to the bimetallic controversy and the theory of interest. *Publications of the American Economic Association 11*(4), 331–442.

Fleckenstein, M., F. A. Longstaff, and H. Lustig (2017, 02). Deflation Risk. *The Review of Financial Studies 30*(8), 2719–2760.

Giannone, D., M. Lenza, and G. E. Primiceri (2019). Priors for the long run. *Journal of the American Statistical Association 114*(526), 565–580.

Harvey, A. C. (1990). *Forecasting, Structural Time Series Models and the Kalman Filter.* Cambridge University Press.

Haubrich, J., G. Pennacchi, and P. Ritchken (2012). Inflation expectations, real rates, and risk premia: Evidence from inflation swaps. *Review of Financial Studies 25*(5), 1588–1629.

Holston, K., T. Laubach, and J. C. Williams (2017). Measuring the natural rate of interest: International trends and determinants. *Journal of International Economics 108*, S59–S75. 39th Annual NBER International Seminar on Macroeconomics.

Hordahl, P. and O. Tristani (2014, September). Inflation Risk Premia in the Euro Area and the United States. *International Journal of Central Banking 10*(3), 1–47.

Joslin, S., A. Le, and K. J. Singleton (2013, 08). JFEC Invited Paper: Gaussian Macro-Finance Term Structure Models with Lags. *Journal of Financial Econometrics 11*(4), 581–609.

Joslin, S., K. Singleton, and H. Zhu (2011). A new perspective on gaussian dynamic term structure models. *Review of Financial Studies 24*(3), 926–970.

Joyce, M. A., P. Lildholdt, and S. Sorensen (2010). Extracting inflation expectations and inflation risk premia from the term structure: A joint model of the uk nominal and real yield curves. *Journal of Banking and Finance 34*(2), 281–294.

Kozicki, S. and P. Tinsley (2001). Shifting endpoints in the term structure of interest rates. *Journal of Monetary Economics 47*(3), 613–652.

Liu, Y. and J. C. Wu (2021). Reconstructing the yield curve. *Journal of Financial Economics 142*(3), 1395–1425.

Stevens, A. and J. Wauters (2021, August). Is euro area lowflation here to stay? Insights from a time-varying parameter model with survey data. *Journal of Applied Econometrics 36*(5), 566–586.

Tibshirani, R. (1996). Regression shrinkage and selection via the lasso. *Journal of the Royal Statistical Society: Series B (Methodological) 58*(1), 267–288.